ENGINEERING RESEARCH INSTITUTE
THE UNIVERSITY OF MICHIGAN
ANN ARBOR

EVALUATION OF THE HUDSON ENGINEERING COMPANY AIR-TEST BOND-RESISTANCE APPARATUS

Report No. 43

Edwin H. Young

Assistant Professor of Chemical and Metallurgical Engineering

Dennis J. Ward
James R. Wall
Marvin L. Katz
William F. Conroy
Walter R. Gutchess

Research Assistants

Project 1592

WOLVERINE TUBE DIVISION
CALUMET AND HECLA, INCORPORATED
DETROIT, MICHIGAN

May 1956

TABLE OF CONTENTS

TABLE OF CONTENTS (Concl.)

LIST OF TABLES

LIST OF FIGURES

OBJECTIVE

The purpose of this investigation was to evaluate the Hudson air-test apparatus as a production-control device for bimetal high-fin tubes.

ABSTRACT

The results of this investigation indicate that (1) the Hudson air-test apparatus can be used as a production-control device if the sensitivity of the unit is acceptable and (2) a testing device having considerably greater sensitivity would permit closer production control of low-bond-resistance tubes.

I. INTRODUCTION

Bimetal integral aluminum spiral-finned tubes have found wide usage in a variety of heat transfer applications. For certain applications a liner is placed inside the aluminum finned tube. This may be done to protect the tube from corrosion or erosion. A small air gap, oil film, or other foreign matter between the liner and the finned-tube wall would cause an additional resistance to heat transfer. This additional resistance to heat transfer is sometimes referred to as "bond resistance" or "contact resistance."

In heat transfer applications involving multilayer materials, no allowance is normally made for the interface resistance to heat transfer where the materials are in contact. Such a procedure is valid in the cases where the materials themselves have low thermal conductivities and are controlling the performance of the system. The assumption of no interface resistance presupposes the absence of gases or vacant spaces caused by blow holes, bubbles, rough surfaces, etc., which are likely to be present where two solid surfaces are brought into contact.[1*] Traces of poorly conducting materials between metals, such as oxide films or air, cause abrupt drops in temperature.

Figure 1 schematically presents the heat flow pattern that exists at the interface of two metals in contact. The metal surfaces are actually in contact over a limited area. The void space may contain air, oil, or other foreign material. As indicated in the figure, when heat flows from one surface to the other the flux lines converge in the region of the area of contact. The area of contact can be increased by pressing the surfaces together. Pressing the surfaces together may cause the metal, at the point of contact, to be either elastically or plastically deformed. Several investigators have studied the effect of pressure on the contact surface area and on the heat transfer rate.[2-7,9] The mathematical theory of elasticity and plasticity has been used to explain some of the heat transfer phenomena resulting from pressing the surfaces together.[2,6]

*References are given on page 42.

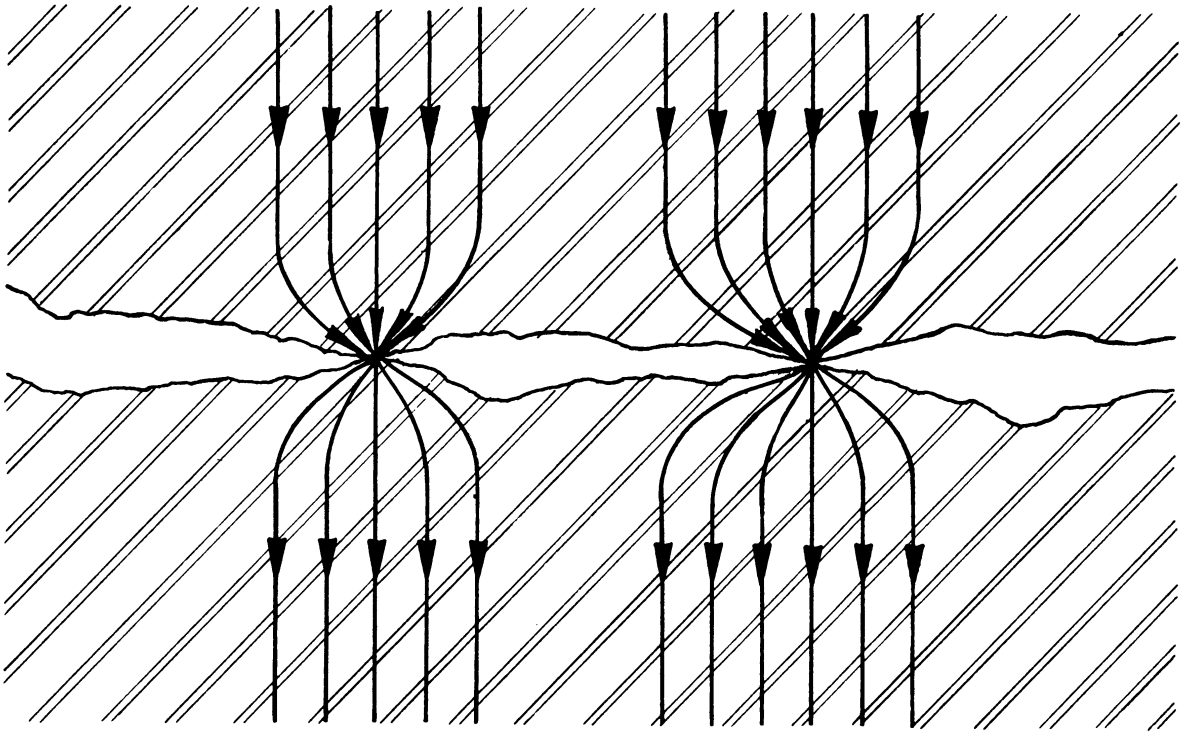

Fig. 1. Schematic representation of heat flow across metallic contact areas.

SURVEY OF PERTINENT PUBLISHED PAPERS

The thermal resistance of metallic contacts apparently has been under investigation for quite a number of years. The problem was present in electrical switches[3,7] and in the dissipation of combustion heat in lined cylinder blocks.[2] One of the earliest investigations reported concerned the heat contact between different parts of a cryogenic apparatus.[4]. The thermal conductance between two clean metallic surfaces in contact in a vacuum is of importance in the design of such an apparatus. Jacobs and Starr[4] studied the thermal conductances between various clean surfaces in a high vacuum. The conductances were studied as a function of pressure and the investigation was limited to good heat conductors such as copper, silver, and gold. Since the quality and flatness of the surfaces considerably affected their results, they polished the surfaces to approximately optical flatness. They then found that the slightest trace of grease at the interface resulted in an increased conductance at room temperature and a decrease in conductance at low temperatures where the grease became hard. For copper against copper they found a linear relationship between thermal conductance and pressure at the interface. The following relationship fits their data:

$$K = 0.08\,P\,, \qquad (1)$$

where

K = thermal conductance, watts/cm^2 °C and
P = contact pressure, Kg/cm^2.

This equation indicates that in the case of optically smooth copper surfaces, doubling the interface contact pressure between the contacts doubles the thermal conductance.

Weills and Ryder[2] studied the thermal resistance of dry and oil-filled interfaces between flat surfaces of various metals. The experimental apparatus used consisted of two test blocks 3 in. in diameter by 3 in. long, stacked axially one on another between the platens of a hydraulic press. The upper block was inductivily heated and the lower block watercooled. The thermal conductance was obtained from measurements of heat flow and temperature gradient through the blocks. The effects of temperature, pressure, and surface finish were studied. The investigators found that the thermal resistance at the interface is decreased by increasing the temperature and pressure, by the inclusion of oil, or by plating the surfaces with a soft metal. As a result of their experiments, Weills and Ryder made the following conclusions:

1. The thermal conductance of a dry joint increases with pressure, linearly for steel, and generally exponentially for aluminum and bronze.

2. The thermal resistance of both dry and oil-filled joints decreases with a decrease in roughness of the surfaces.

3. At a given temperature, pressure, and roughness, the thermal resistance of both dry and oil-filled joints decreases in the order of steel, bronze, and aluminum.

4. The thermal resistance of a dry joint decreases as the temperature increases. For oil-filled joints, no consistent relationship was found.

5. The thermal resistance is about one-half as great for oil-filled joints as for dry joints at 10 psi. The effect of the oil decreases at higher pressures. The thermal resistance is decreased by copper plating one surface of a steel joint.

6. A hysteresis-like loop in the thermal conductance-pressure relation is obtained when the pressure is decreased following an increase in pressure.

7. The presence of a film of oxide or other foreign material of low thermal conductivity could contribute to the thermal resistance of a joint. However, except for very low interface pressure, the oxide resistance appears to account for only a small part of the total resistance.

The investigators also indicated that they believe that the area in metallic contact is directly proportional to the load during plastic deformation and to the two-thirds power of the load during elastic deformation. This

opinion is based on the mathematical theory of elasticity.[8]

Centinkale and Fishenden[6] considered the plastic flow of the metal at the interface when the surfaces are pressed together. These investigators concluded that when pressure is applied to the contact, the softer of the two metals will plastically flow until the average pressure at the contact interface is equal to the average resistance per unit area against indentation (Meyer hardness). If the pressure is subsequently reduced, the metallic flow is elastic and the area of contact is a function of the pressure to the two-thirds power.

Kouwenhoven and Potter[9] studied the thermal conductance of steel-to-steel contacts under various conditions. The effects of pressure, temperature, and surface roughness were explored. The investigators assumed that the surface consisted of a series of parallel isosceles trapezoid ridges ("like a plowed field"). As the pressure at the interface is increased, the trapezoids are assumed to crush, increasing the contact area. They presented the following relationships for predicting the increase in contact area as a function of the original contact area and the relative height of the trapezoids:

$$A_f = A_o + 2\ell + 2\sqrt{\ell A_o + \ell^2}, \qquad (2)$$

where

A_f = final contact area,

A_o = initial contact area, and

ℓ = decrease in trapezoid height as a result of pressure.

Since A is the area of contact, 1/A is a measure of the resistance to heat flow. The influence of pressure was found to be greater for rough surfaces. In general, Kouwenhoven and Potter's results agreed with those of Weills and Ryder.[2]

Brunot and Buckland[10] investigated the thermal conductance of blocks of laminated steel. They also found that the effect of pressure was considerably greater in the case of rough surfaces and concluded that contact resistances vary widely depending on smoothness, contact pressure, thermal conductivity of the metal, and thermal conductivity of the material between the metal surfaces.

The published data referred to above form a useful basis for the investigation of bond resistance to heat transfer in bimetal tubes. The concept of treating the effect of the bond as a separate resistance to heat transfer is a fundamentally correct approach to the problem. The reciprocal

of the bond resistance is the conductance of the bond.

PROBLEM UNDER INVESTIGATION

The Hudson Engineering Company designed and built a unit to test the performance of finned tubes. A copy of the blueprints used to build this unit was obtained from that company. A similar unit was built at The University of Michigan for evaluation by the project.

The evaluation of this unit involves the determination of its ability to detect and measure in a reproducible manner the bond resistance of a tube. The sensitivity of the device to differences in bond resistance between different tubes is an important control criterion of the unit.

II. PREVIOUS WORK ON BIMETAL FINNED TUBES

Project Reports No. 26 and No. 34, entitled "Development of a Test for Bond Resistance to Heat Transfer in Bimetal Finned Tubes" and "Effect of Root Wall Thickness on Bond Resistance to Heat Transfer of Bimetal Tubes," respectively describe a test method for bond resistance. In this method water was circulated by natural convection on the outside of the finned tube being tested, and steam was condensed or water was pumped inside the tube.

The main conclusions reached in these reports were:

1. The described test method was suitable for measuring bond resistance.
2. Root-wall thickness apparently had no effect on bond resistance.

III. DESCRIPTION OF AIR-TEST APPARATUS

A schematic diagram of the test equipment is presented in Fig. 2. The test unit essentially consists of a centrifugal blower for blowing air perpendicular to a steam-heated finned tube. An American Blower type 75H was used for this purpose. Provisions were made for measuring the inlet-steam temperature and pressure, and the inlet- and outlet-air temperatures. A Taylor vane-type anemometer, model No. A413, was used to measure the discharge-air velocity. To prevent the accumulation of noncondensables, steam was continuously bled from the system.

Straightening vanes were placed between the blower and the tubes

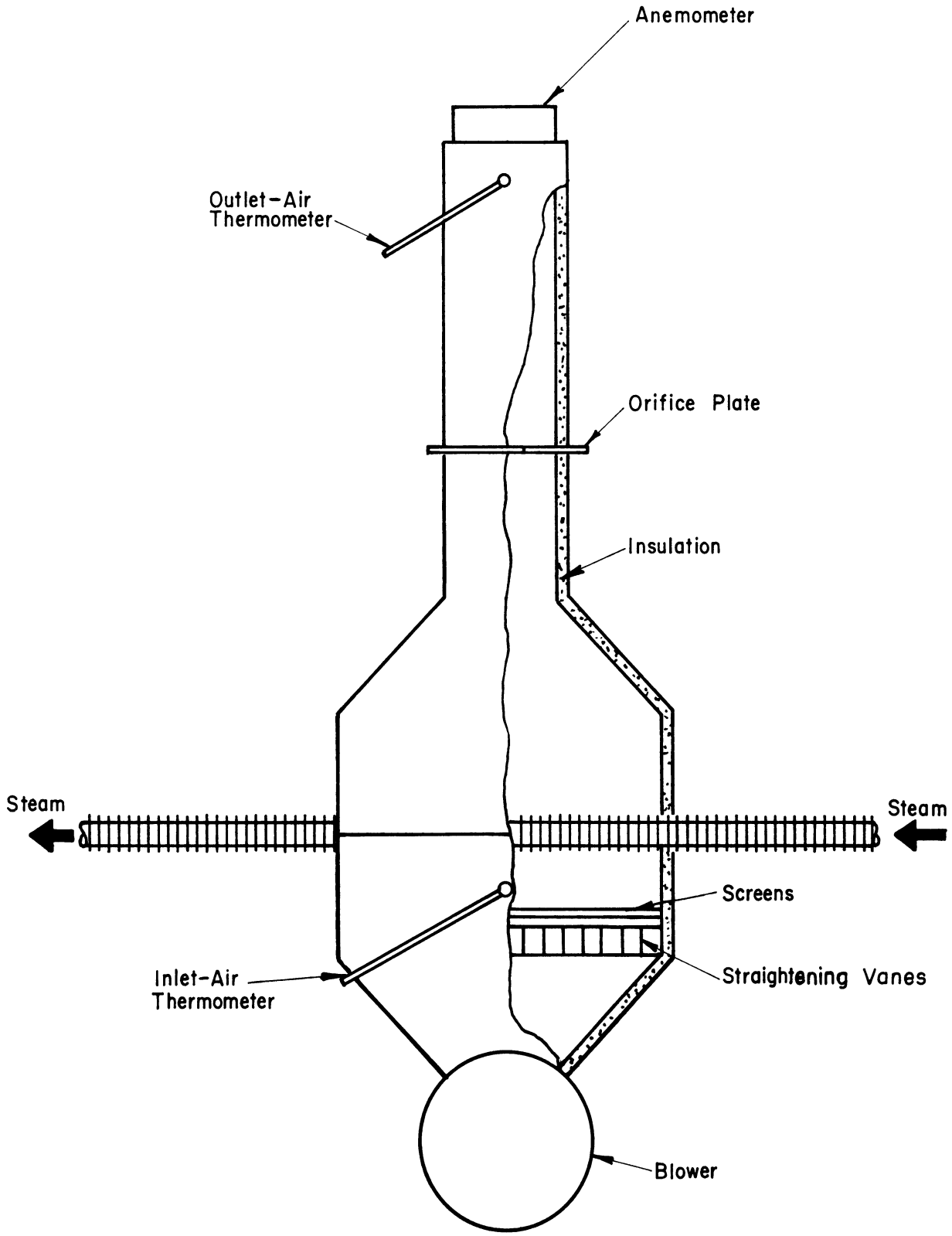

Fig. 2. Schematic diagram of test apparatus.

being tested in order to remove large-scale turbulence created by the blower. The inlet-air thermometer was placed above the vanes and about 6 in. below the finned tube. The outlet-air temperatures were measured using a thermometer placed above the orifice plate but below the anemometer.

The thermometers were calibrated against a thermometer calibrated by the Bureau of Standards. The steam-pressure gage was calibrated against a 100-in. Merriam mercury manometer.

IV. OPERATIONAL PROCEDURE

Steam was first purged at a rapid rate through the tube to remove inside fouling. The pressure was then set at 10 psig for all experimental runs. Approximately 20 min were allowed for the equipment to reach equilibrium. A stopwatch and the anemometer were then started simultaneously, after which inlet- and outlet-air temperatures, and steam-temperature and -pressure readings were recorded at 1-min intervals for a total of five readings. The stopwatch and anemometer were then simultaneously stopped and their readings recorded.

Steam was then again purged at a rapid rate through the tube to remove any condensate in the tube. The test procedure described above was repeated and the temperature data were compared with the previous measurements to ascertain that equilibrium had been reached. Typical test data are given in Table I.

TABLE I

TYPICAL TEST DATA

Run No. 414

Date of Run	Tube Designation No. 17
12-20-55	All-aluminum tube

Anemometer reading = 9100 ft
Anemometer time = 5 min 4.9 sec

Inlet-air thermometer reading = 27.06°C
Calibration correction to thermometer = -0.09°C
Correction due to radiation and other effects = -1.00°C
Actual inlet-air temperature = 25.97°C = 78.75°F

Outlet-air thermometer reading = 48.66°C
Calibration correction to thermometer = -0.03°C
Actual outlet-air temperature = 48.63°C = 119.55°F

Steam pressure = 10 psig
Barometer reading = 752.0 mm Hg
Barometer temperature = 18°C

V. THEORETICAL CONSIDERATIONS

The overall coefficient of heat transfer is defined as

$$Q = U_O A_O \Delta T_m \ , \qquad (3)$$

where

Q = heat transferred, Btu/hr,

U_O = overall coefficient of heat transfer, Btu/hr/°F/ft^2 based on outside area,

A_O = outside heat transfer area, ft^2, and

ΔT_m = mean-temperature driving force, °F.

The overall coefficient of heat transfer is further defined for bimetal tubes as

$$U_O = \frac{1}{\frac{1}{h'_O} + r_f + r'_O\left(\frac{A_O}{Aeq}\right) + r_m\left(\frac{A_O}{A_m}\right) + r_b\left(\frac{A_O}{A_L}\right) + r_i\left(\frac{A_O}{A_i}\right) + \frac{1}{h_i}\left(\frac{A_O}{A_i}\right)} \ , \qquad (4)$$

where

h'_O = outside film coefficient, Btu/hr/°F/ft^2,

r_f = fin resistance (see Equation 5), Btu/hr/°F/ft^2,

r_m = root-wall metal resistance, Btu/hr/°F/ft^2,

A_m = log mean heat transfer area, ft^2,

r_b = bond resistance, Btu/hr/°F/ft^2,

A_L = outside area of the liner tube, ft^2,

r_i = inside fouling resistance, Btu/hr/°F/ft^2,

A_i = inside heat transfer area of liner tube, ft^2, and

h_i = inside film coefficient, Btu/hr/°F/ft^2.

The fin resistance[11,12] is defined by Equation 5. The derivation of this relationship is given in Appendix A.

$$r_f = \left[\frac{1}{h'_O} + r'_O\right]\left[\frac{1 - E_f}{\frac{A_r}{A_f} + E_f}\right] \ , \qquad (5)$$

where r_o = outside fouling resistance. The fin-resistance concept as presented by Carrier and Anderson[11] is convenient to use where repetitive calculations are encountered. The method is an alternate procedure which can be used in place of that used in previous reports. Following the procedure used in the earlier reports, the overall coefficient of heat transfer would be written as

$$U_o = \frac{1}{\frac{1}{h_o} + r_o + r_m\left(\frac{A_o}{A_m}\right) + r_b\left(\frac{A_o}{A_L}\right) + r_i\left(\frac{A_o}{A_i}\right) + \frac{1}{h_i}\left(\frac{A_o}{A_i}\right)}, \qquad (6)$$

where h_o = outside heat transfer coefficient based on A_o. A comparison of Equation 6 with Equation 4 indicates that the following substitution has been made:

$$\left[\frac{1}{h_o}\right] = \left[\frac{1}{h_o'} + r_f\right]. \qquad (7)$$

The relation between h_o' and h_o is given by

$$h_o' \, Aeq = h_o \, A_o . \qquad (8)$$

The equivalent area is a function of the efficiency of the fin and may be determined by

$$Aeq = A_r + E_f \, A_f , \qquad (9)$$

where

A_r = root area, ft^2,

E_f = fin efficiency, Fig. 3,[13] and

A_f = fin area, ft^2.

In the range of air velocities encountered in the operation of the air test, the values of the air-side coefficient, h_o, vary from 6 to 10. The corresponding fin efficiencies vary from 97% to 92%, respectively. A typical bimetal finned tube has a fin OD of 2.00 in., a root diameter of 1.10 in., and a fin thickness of 0.019 in. The root area, A_r, for such a tube is 0.30 ft^2/ft length of tube. The area of the fin, A_f, is 3.29 ft^2/ft, and A_o is 3.59 ft^2/ft. By Equation 9,

$$Aeq = 0.30 + 3.29 \, E_f$$

for E_f = 0.92%.

$$\therefore \quad Aeq = 0.30 + 3.29 \, (0.92)$$

$$= 3.33 \text{ ft}^2\text{/ft and}$$

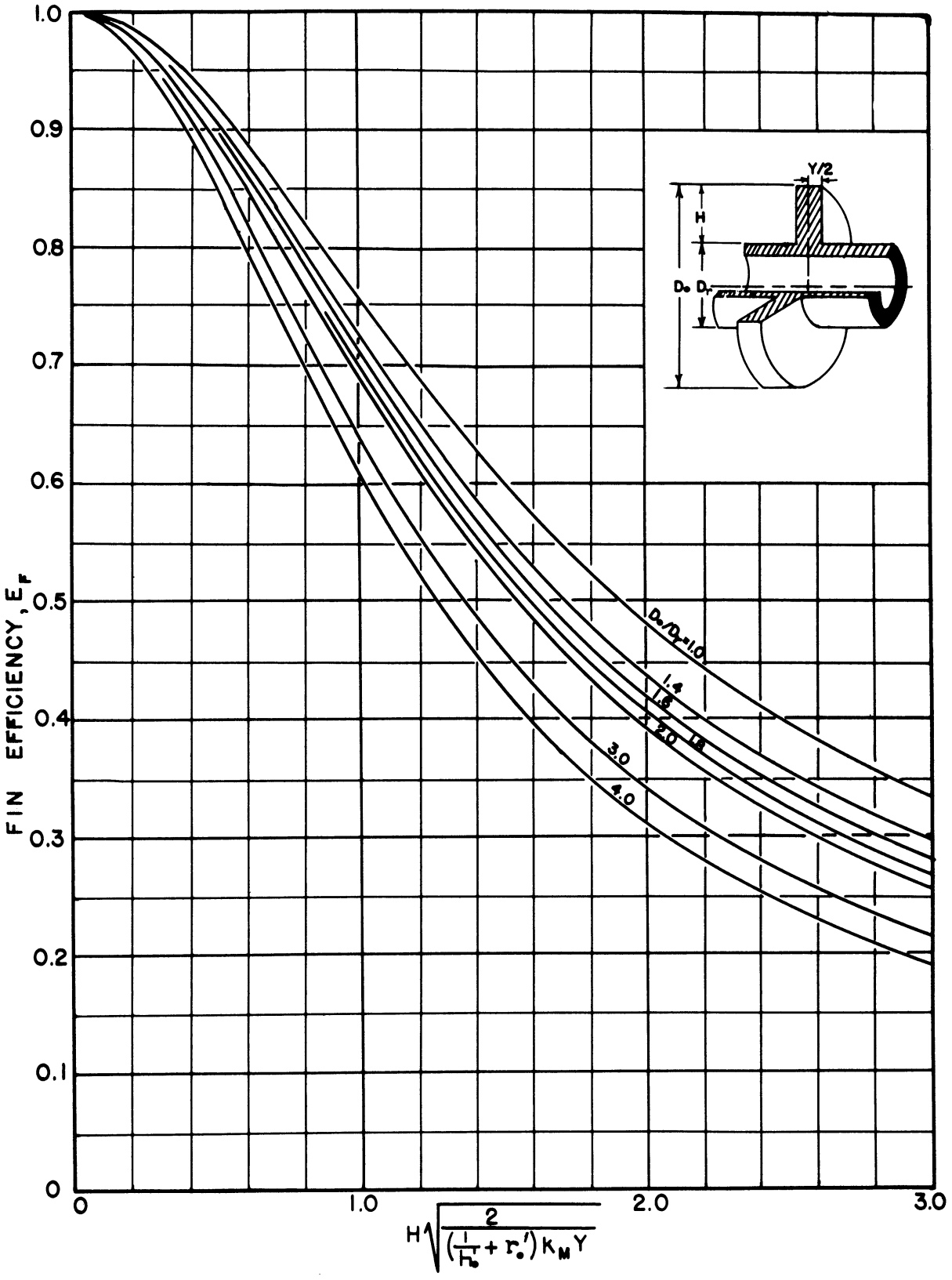

FIGURE 3. EFFICIENCY OF ANNULAR FINS OF CONSTANT THICKNESS

$$\frac{A_o}{Aeq} = \frac{3.59}{3.33} = 1.08$$

For $E_f = 0.97\%$,

$$Aeq = 0.30 + 3.29\ (0.97)$$

$$= 3.49\ ft^2/ft \text{ and}$$

$$\frac{A_o}{Aeq} = \frac{3.59}{3.49} = 1.03.$$

$\therefore$

$h_o' = 1.08\ h_o$ for $E_f = 92\%$ and

$h_o' = 1.03\ h_o$ for $E_f = 97\%$.

A plot of Equation 5 giving the fin resistance, r_f, in terms of h_o', r_o, and fin efficiency, E_f (using Fig. 3), is given in Fig. 4. In order to use this figure, h_o' must be known. In the laboratory experimental research work, h_o is obtained directly. Table II presents the fin efficiencies. equivalent areas, and h_o as a function of h_o' for the tube described in Fig. 4.

TABLE II

h_o' AND h_o FOR FINNED TUBE OF FIG. 4

h_o'	E_f(%)	Aeq	$\frac{Aeq}{A_o}$	r_f	h_o
600	27.5	0.881	0.329	.00382	197.5
400	34.0	1.420	0.396	.00374	158.1
200	47.5	1.862	0.520	.00463	103.8
100	62.5	2.355	0.656	.00523	65.5
50	75.0	2.765	0.772	.00594	38.5
25	86.0	3.130	0.874	.00588	21.8
10	93.0	3.360	0.910	.00684	9.35
0	100.0	3.59	1.000		0

The values of h_o and h_o' given in Table II are plotted for convenience in Fig. 5.

Equation 4 indicates that the overall coefficient of heat transfer is equal to the reciprocal of the sum of the individual resistances to heat

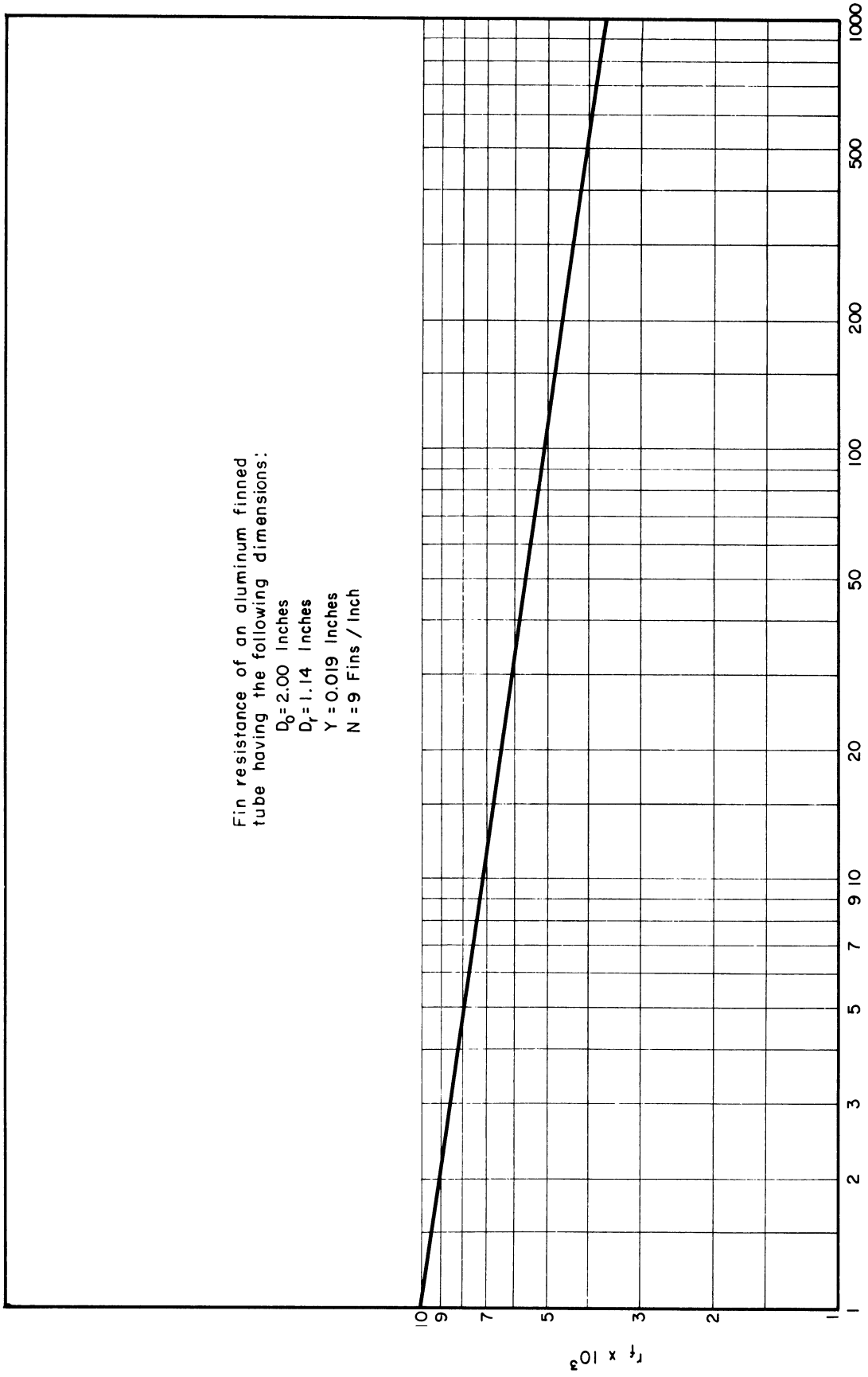

Fig. 4. Fin resistance versus outside coefficient.

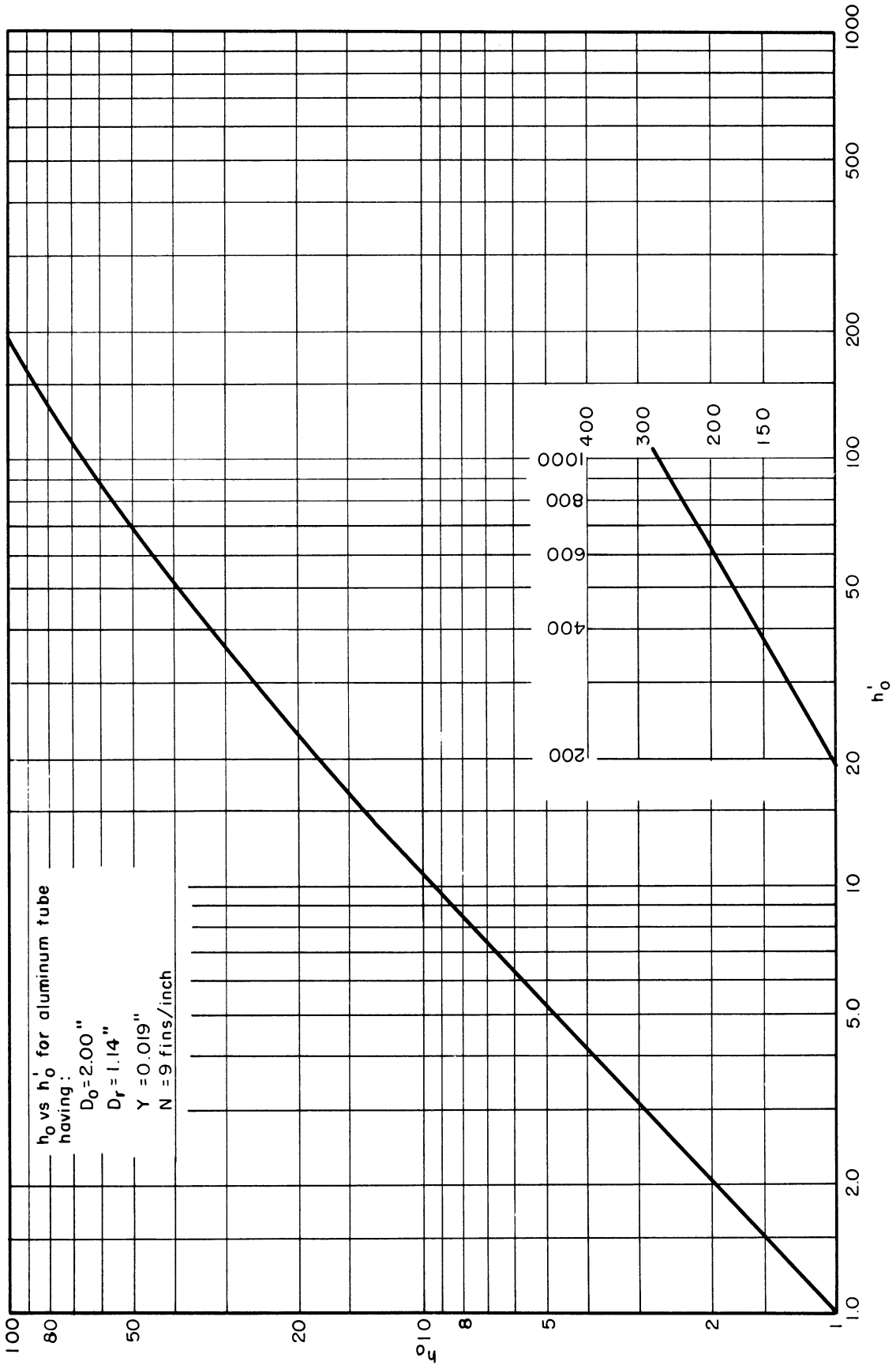

Fig. 5. Calculated values of h_o versus h'_o.

transfer. In the case of the tubes tested, the outside fouling resistance, r_o, and the inside fouling resistance, r_i, were for all practical purposes zero. The new tubes had clean fins and, as described in the previous section, steam was used to clean the inside of the tubes. Therefore, Equation 4 reduces to

$$\frac{1}{U_o} = \frac{1}{h'_o} + r_f + r_m \left(\frac{A_o}{A_n}\right) + r_b \left(\frac{A_o}{A_L}\right) + \frac{1}{h_i}\left(\frac{A_o}{A_i}\right), \qquad (10)$$

where $1/U_o$ = overall resistance to heat transfer, Btu/hr/°F/ft^2. In this simplified case where $r_o = 0$, the abscissa of Fig. 4 becomes h'_o.

In most heat transfer studies, values of U_o are obtained directly. Other resistances or coefficients are calculated by subtracting out known resistances obtained from Wilson plots, wall temperatures, or empirical equations.

From the above equations and discussion it can be seen that if one wishes to study any particular resistance to heat transfer, such as bond resistance, the other resistances involved should be minimized. If this is done, variations in $1/U_o$ will reflect variations in the resistance being studied. If other resistances besides the one being studied are large and also vary, such variations can easily mask the variations of the resistance under study. This subject is developed further in Section XIII of this report.

In the air-test apparatus the velocity of the air past the finned tube affects the outside-air film coefficient of heat transfer. A review of the literature (see Section VI) indicates that the variations in air film coefficients are correlated in the following form:

$$h'_o = aV^b . \qquad (11)$$

The various values of a and b obtained by different investigators are summarized in Section VI.

VI. SUMMARY OF PUBLISHED RELATIONSHIPS FOR AIR FILM COEFFICIENTS

A survey of the technical literature since 1942 indicates the following equations for air-side coefficients for tubes:

1. Norris and Spofford:[14]

$$h_o' = C_1 (V_{max})^{0.5} . \quad (12)$$

2. Lemmon, Colburn, and Nottage:[15]

$$U_o = C_2 (V_{max})^{0.53} . \quad (13)$$

3. Jameson[16] (for various finned tubes):

$$h_o' = C_3 (V_{max})^{0.60} , \quad (14)$$

$$h_o' = C_4 (V_{max})^{0.69} , \quad (15)$$

$$h_o' = C_5 (V_{max})^{0.675} , \quad (16)$$

$$h_o' = C_6 (V_{max})^{0.655} , \quad (17)$$

$$h_o' = C_7 (V_{max})^{0.718} , \text{ and} \quad (18)$$

$$h_o' = C_8 (V_{max})^{0.666} . \quad (19)$$

4. Kays and London[17] (for various finned tubes):

$$\text{Fig. 92, } h_o' = C_9 (V_{max})^{0.8} , \quad (20)$$

$$\text{Fig. 93, } h_o' = C_{10} (V_{max})^{0.763} , \quad (21)$$

$$\text{Fig. 94, } h_o' = C_{11} (V_{max})^{0.76} , \quad (22)$$

$$\text{Fig. 95, } h_o' = C_{12} (V_{max})^{0.59} , \text{ and} \quad (23)$$

$$\text{Fig. 96, } h_o' = C_{13} (V_{max})^{0.72} . \quad (24)$$

5. Katz, Beatty, and Foust:[18]

$$U_o = C_{14} (V_{max})^{0.53} . \quad (25)$$

6. Schmidt[19] (first row of finned tubes in a tube bank):

$$h_o' = C_{15} (V_{max})^{0.29} , \quad (26)$$

$$h_o' = C_{16} (V_{max})^{0.47} , \quad (27)$$

$$h_o' = C_{17} (V_{max})^{0.41} , \quad (28)$$

$$h_o' = C_{18} (V_{max})^{0.525} , \text{ and} \quad (29)$$

$$h_o' = C_{19} (V_{max})^{0.44} , \quad (30)$$

An examination of Equations 12 through 30 indicates that the power (exponent) on the maximum velocity varies from 0.29 to 0.8. Most of the exponent values appear to be in the neighborhood of 0.65. It should be pointed out that the above equations do not contain the value of the constants C_1 through C_{19} because the data were obtained on a wide variety of tubes in various test arrangements and were reported in many forms. Many of the exponents reported above were computed from the published data and curves.

VII. ANEMOMETER DUCT CORRECTION FACTOR

In the early stages of this investigation it was observed that the air film coefficients obtained on the air-test apparatus were considerably higher than those published in the Katz, Beatty, and Foust article[18] and in the correlation report.[20] Some of the data published in the correlation report were for tube banks one row and two rows deep. The Katz-Beatty-Foust data were obtained on single tubes, one-row banks, and two-row banks. As a result of this discrepancy an investigation on the influence of a 4-in. duct on the Birams type vane anemometer was undertaken. Report No. 37[21] was issued as a result of this investigation. Figure 3 of that report (p. 12) indicates that the actual amount of air flowing through the 4-in. duct is 66% of that indicated by the anemometer.

Early air-test results (using the 66% duct correction factor) indicated that the exponent on the velocity term for all-aluminum tubes was about 0.35 This value was considerably lower than that expected, since the literature indicated that the probable value would be in the neighborhood of 0.6. As a result of this situation an independent check of the anemometer correction factor for a 4-in. duct was made with the anemometer in the air-test apparatus. Steam condensate was collected and air-side and steam-side heat balances were obtained. The results verified the 66% correction factor. The actual value obtained by this latter method was 65.3%. Figure 6 presents the test curve. The test data are summarized in Appendix B.

It was concluded that the duct correction factor is an essential correction that must be taken into consideration in analyzing the air-test data. It was also concluded that the low value of the velocity exponent could not be explained by an error in the anemometer duct correction factor. Two other possible factors could explain all or part of the low exponent. These are: (a) thermometer error due to radiation or other factors; (b) air-turbulence factors. These are discussed in Sections VIII and IX of this report.

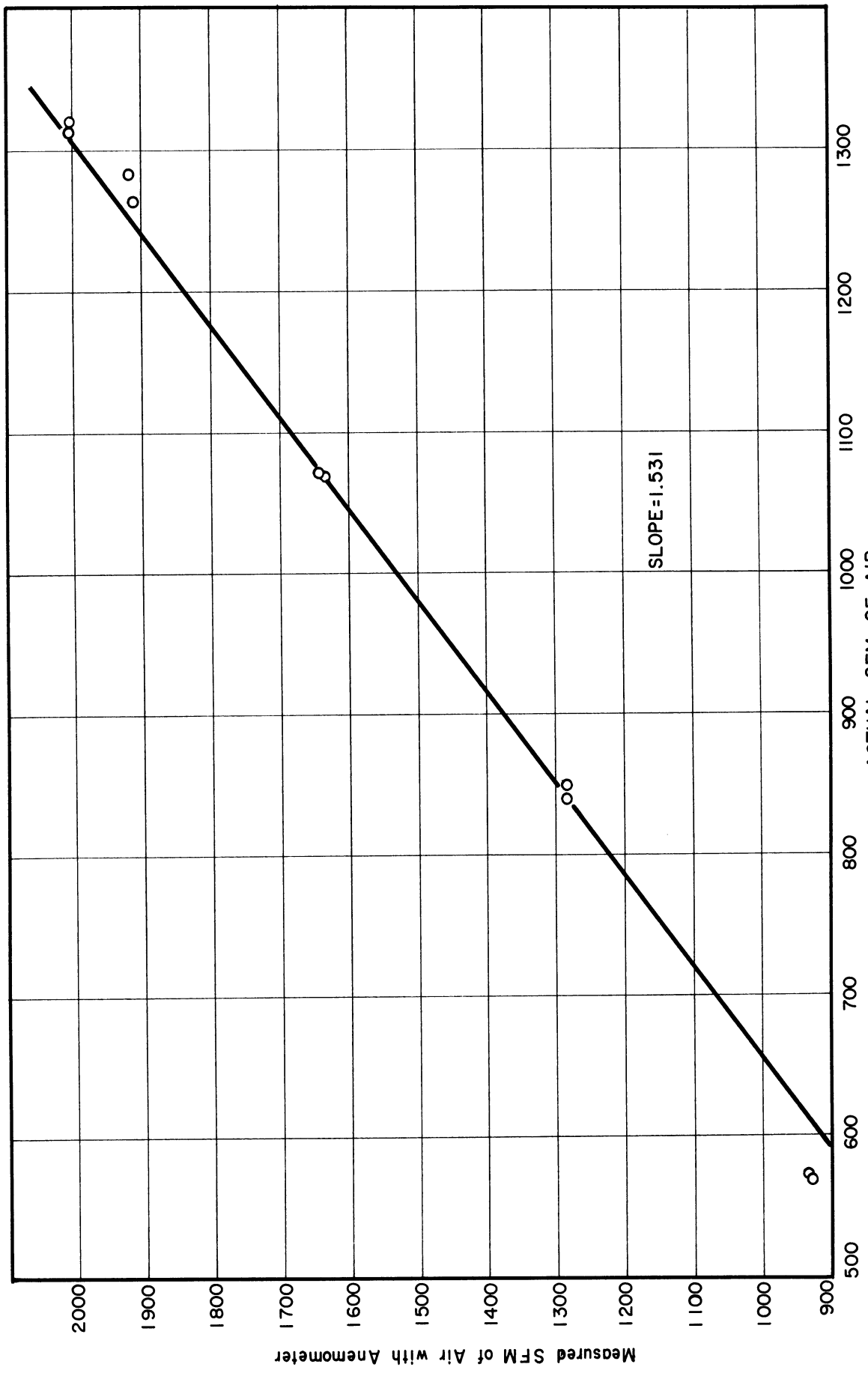

Fig. 6. Calibration of anemometer in four-inch duct.

VIII. THERMOMETER CORRECTION FACTORS

The possibility of radiation from the hot finned tube to the inlet-air thermometer was experimentally investigated. This was done in the following manner. A second inlet-air thermometer was placed in the ambient-air stream going to the blower. It was observed that there existed a significant difference between the temperature readings.

It was apparent that part or all of this difference might be accounted for by the energy added to the inlet-air stream by the blower. If only part of the difference was due to the blower, the remaining portion would be due to radiation or possibly to conduction of heat from the test tube to the wall of the apparatus and finally by convection to the air in the neighborhood of the thermometer.

To determine the blower effect, the tube was not heated and the air thermometers were read with varying air velocities. A calibration curve was established giving the temperature rise of the air due to the blower as a function of the air velocity past the tube. Analogous test data were obtained for the condition in which the tube was heated. The results of these two series of tests are presented in Fig. 7 and the test data are tabulated in Appendix C.

It was concluded that these correction factors are significant and must be taken into account when analyzing air-test data. This situation could be avoided by redesigning the air-test apparatus so as to relocate the inlet-air thermometer in such a manner that no such correction is required.

IX. BLOWER TURBULENCE EFFECTS

The centrifugal blower used in the air-test apparatus tends to discharge the air against the back wall of the duct going to the tube. As indicated in Section III of this report, straightening vanes were installed between the blower discharge and the tube being tested. These straightening vanes were of the "egg-crate" variety.

Discussions with professors of fluid dynamics in both the Engineering Mechanics and the Aeronautical Engineering Departments indicated that the straightening vanes were undoubtedly ineffective in removing all of the centrifugal blower effects. Further discussions with the above personnel indicated that one or two screen grids would be required to smooth out blower disturbances.

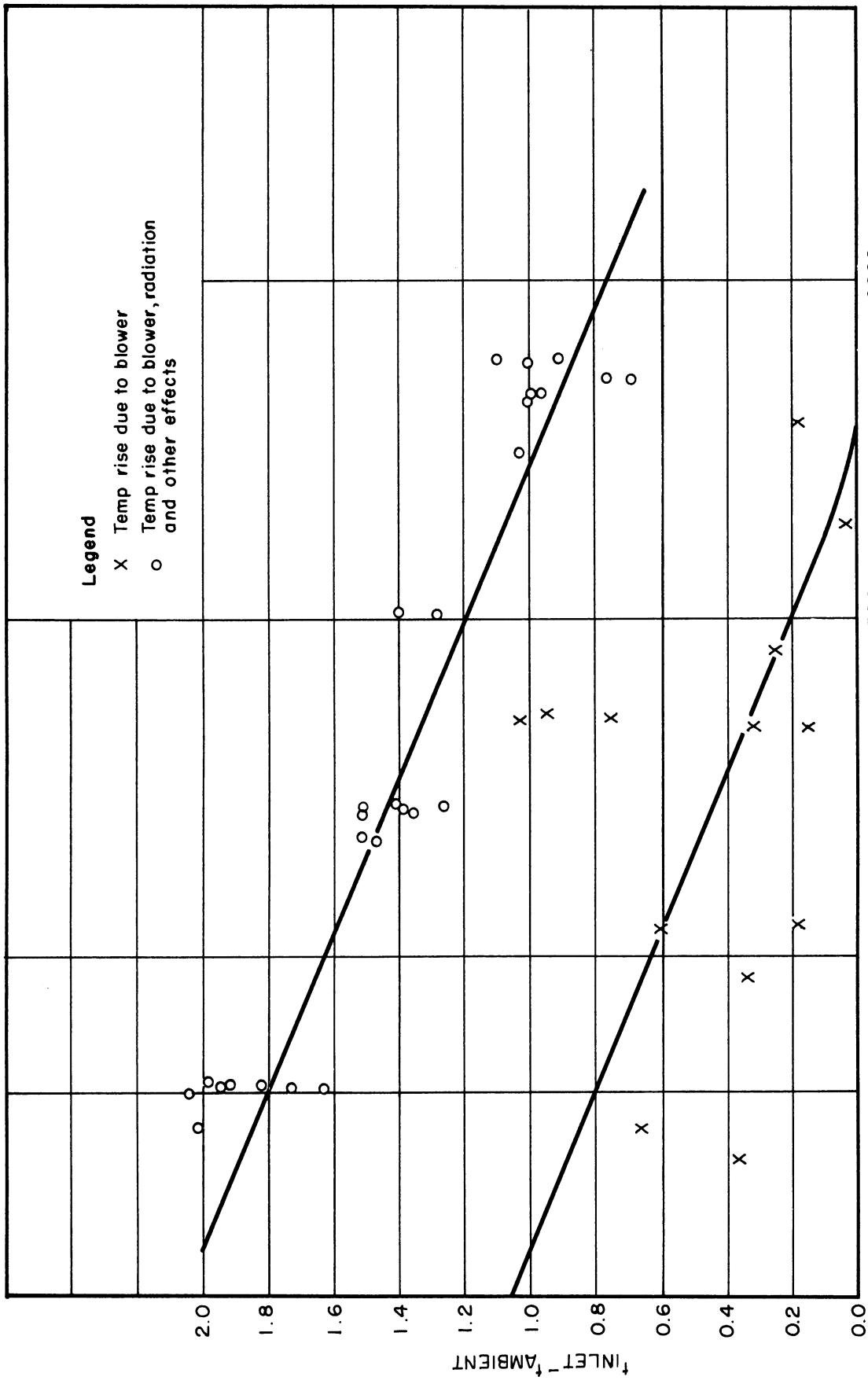

Fig. 7. Temperature rise of the inlet air due to blower, radiation, and other effects.

Initially one 30-mesh screen was inserted above the straightening vanes. Later a second 30-mesh screen was inserted about one inch above the first screen.

The data obtained from an all-aluminum tube in the air-test apparatus with no screens, one screen, and two screens, (inserted as described above) are tabulated in Appendix D. The data are presented graphically in Fig. 8 where the reciprocal of the overall heat transfer coefficient ($1/U_o$) is plotted vs the reciprocal of the maximum velocity to the 0.4 power. The power on the velocity was determined from all of the all-aluminum test data and is described in Section XI. The data presented on Fig. 8 were obtained from two separate series of tests. A separate series of tests indicated that it is necessary to clean thoroughly the inside of the tube prior to testing in order to obtain reproducible results. The cleaning was accomplished by blowing live steam through the inside of the tube for about one-half hour. Since this cleaning procedure had not been used on the tube in the initial test measurements made to determine the effects of the screen, a second series of tests were run with an all-aluminum tube cleaned on the inside in the above manner to check the effects of the screens on the tube performance. The results of the second series, also presented on Fig. 8, indicate that the first tube was fouled during the runs made with no screens present in the apparatus. From the data in Fig. 8 it appears that the fouling probably present on the inside of the tube was essentially removed during or following the tests made with no screens present, as it does not appear significant in the one-screen and two-screen data.

The effect of the screens on the outside-air film coefficient is presented in Fig. 9 where the outside-air film coefficient is plotted vs the maximum air velocity on logarithmic coordinates. As shown on this figure, one effect of the screens is to reduce the outside coefficient 11.5%.

The use of screens between the blower and the tube being tested tends to level out the uneven disturbances created by the blower. Since the flow characteristics produced by different blowers would in general not be the same, some method must be used to eliminate blower effects in order to obtain comparable results between air-test apparatuses using different blowers. The use of screens can accomplish this purpose.

X. TEST DATA AND CALCULATION PROCEDURE

TEST DATA

The test data taken on all-aluminum and bimetal tubes in the air-test apparatus consisted of the inlet- and outlet-air temperatures, the anemometer reading and anemometer time, and steam and atmospheric pressures. Typical test

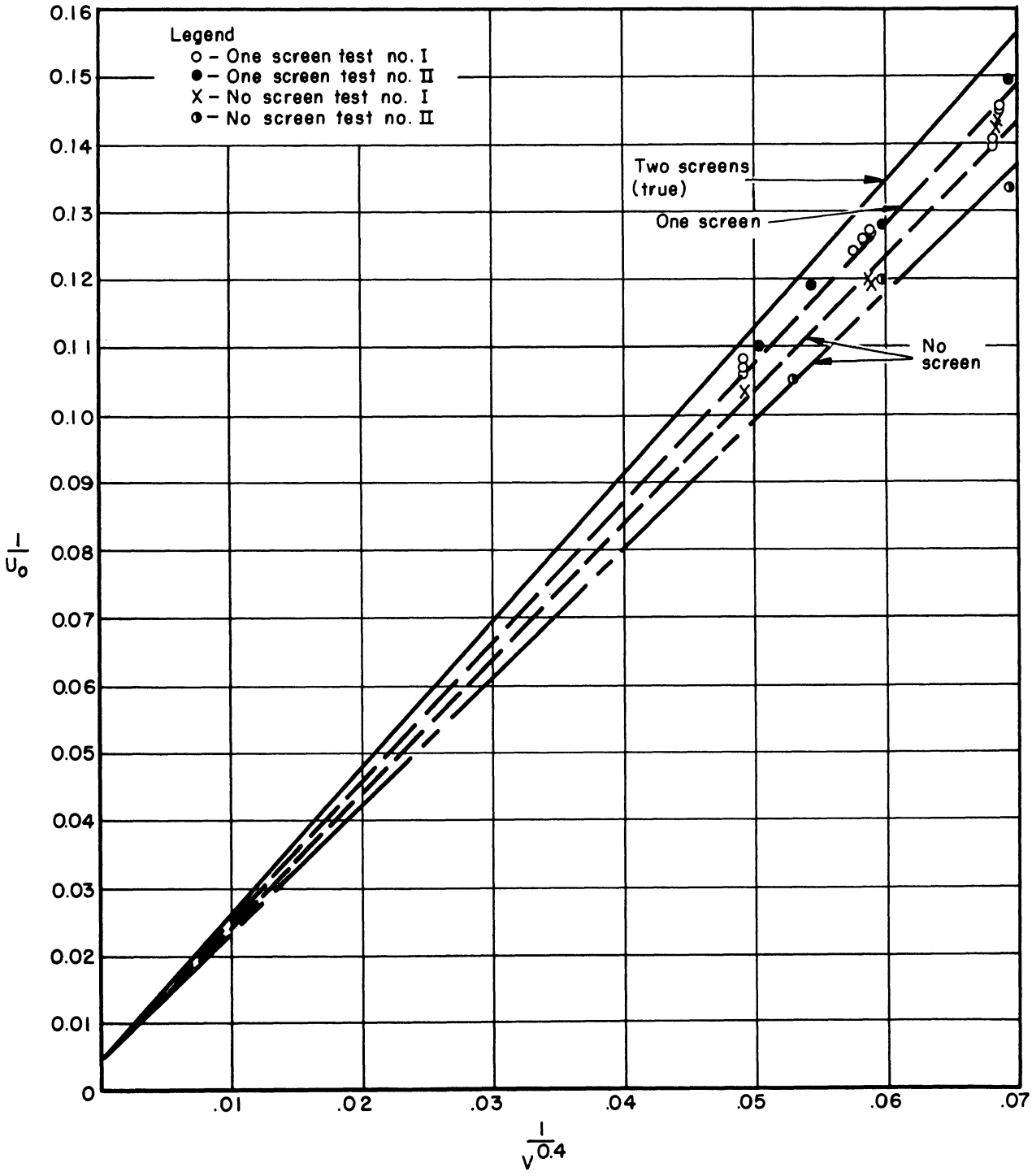

Fig. 8. Effect of screens on performance of tubes.

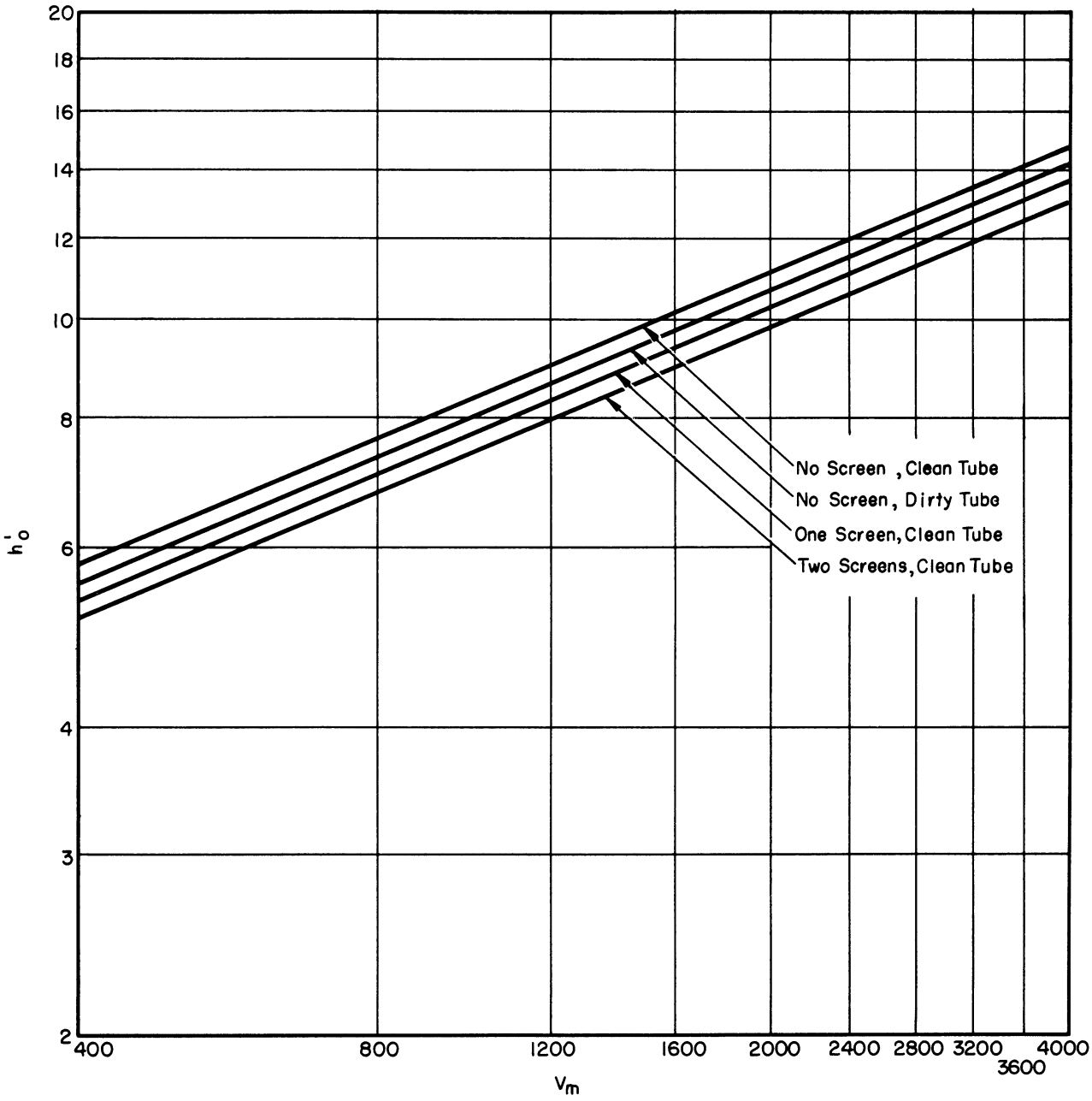

Fig. 9. Effect of screens on the outside coefficient.

data obtained on an all-aluminum tube (No. 16) are given in Table III. Table IV includes typical test data obtained on a bimetallic tube (No. 36). As can be noted from a comparison of Tables III and IV, the measurements taken were the same for both types of tubes, differing only in the experimental values obtained.

A summary of all of the all-aluminum test data for this report is given in Appendix E. Appendix F contains a summary of the bimetallic-tube test data. The test data obtained in the earlier runs without two screens were not used in this evaluation report.

TABLE III

TYPICAL ALL-ALUMINUM-TUBE TEST DATA

Tube No. 16 Run No. 481

Barometer reading = 732.2 mm Hg
Barometer temperature = 20.2°C

Orifice size = 4 in.
Anemometer reading = 9200 ft
Anemometer time = 4 min, 21.8 sec

Inlet-air thermometer reading	=	28.98°C
Correction for radiation and other effects	=	-1.00°C
Thermometer calibration	=	+0.07
Inlet-air temperature	=	28.05°C
	=	82.50°F
Outlet-air thermometer reading	=	48.73°C
Thermometer calibration	=	-0.04°C
Outlet-air temperature	=	48.69°C
	=	119.65°F

Steam pressure = 10 psig

CALCULATION PROCEDURES

Four different calculation procedures had been used at one time or another to analyze the air-test data. The four methods have been referred to as (1) short form of calculation, (2) modified short form, (3) long form, and (4) modified long form. Sample calculations for each of the above procedures are given in Appendix G for Run No. 481. The results of these calculations are given in Table V.

The differences among the four calculation procedures are as follows:

TABLE IV

TYPICAL BIMETALLIC-TUBE TEST DATA

Tube No. 36 Run No. 508
Barometer reading = 720.8 mm Hg
Barometer temperature = 25.8°C

Orifice size = 4 in.
Anemometer reading = 8995 ft
Anemometer time = 3 min, 57.7 sec

Inlet-air thermometer reading	=	30.80°C
Correction for radiation and other effects	=	-1.00°C
Thermometer calibration	=	+0.09°C
Inlet-air temperature	=	29.89°C
	=	85.8°F

Outlet-air thermometer reading	=	47.90°C
Thermometer calibration	=	-0.03°C
Outlet-air temperature	=	47.87°C
	=	118.1°F

Steam pressure = 10 psig
Steam temperature = 114.1°C = 237.4°F

TABLE V

COMPARISON OF CALCULATED RESULTS OF RUN NO. 481

	Calculation Procedure			
	Short Form	Modified Short Form	Long Form	Modified Long Form
V_{face}	980	646	672	672
V_{max}	---	---	1790	1790
U_o (liner OD)	174.5	120.5	118.5	124.8
U_o (outside)	---	---	8.68	9.13
h_o (liner OD)*	205	134	131.5	139.5

*Calculated assuming all resistances except air film equal 0.00085, based on liner area.

1. The short form of calculation does not take into account (a) the density correction on the anemometer, (b) the effects of the duct on the anemometer, (c) corrections on the inlet-air thermometer due to radiation and other effects, or (d) differences in tube geometry.

2. The modified short form of calculation is the same as (1) above except that the effect of the duct on the anemometer reading is taken into account.

3. The long form of calculation is the same as (1) above except that items (a), (b), and (d) are taken into account. No correction is made on the inlet thermometer for radiation and other effects.

4. The modified long form of calculation takes into account all four (a, b, c, and d) of the above factors.

As indicated in Table V, significant differences can exist among the results obtained from the four procedures. The modified long-form type of calculation is believed to give the most significant heat transfer result. This method of computation was used to compute all overall coefficients given in this report.

XI. ANALYSIS OF ALL-ALUMINUM-TUBE DATA

The overall coefficient of heat transfer can be computed using the data given in Appendix E by Equation 3, making proper allowance for anemometer and inlet-air-temperature corrections. The overall coefficient of heat transfer is related to the individual resistances by Equation 4. Equation 4 can be rearranged to give

$$\frac{1}{U_o} = \frac{1}{h_o'} + r_f + r_o' \left(\frac{A_o}{A_{eq}}\right) + r_m \left(\frac{A_o}{A_m}\right) + r_b \left(\frac{A_o}{A_L}\right) + r_i \left(\frac{A_o}{A_i}\right) + \frac{1}{h_i} \left(\frac{A_o}{A_i}\right) \qquad (31)$$

For an all-aluminum tube, the bond resistance, r_b is zero. Assuming no fouling on the inside and outside of the tube ($r_i = r_o' = 0$), Equation 31 reduces to

$$\frac{1}{U_o} = \frac{1}{h_o'} + r_f + r_m \left(\frac{A_o}{A_m}\right) + \frac{1}{h_i} \left(\frac{A_o}{A_i}\right) . \qquad (32)$$

The outside coefficient h_o' is correlated by use of an equation of the following form:

$$h_o' = c\, V_{max}^{b} , \qquad (11)$$

where

c = a constant, and
b = a constant.

Equation 11 can be substituted into Equation 32 to give

$$\frac{1}{U_o} = \frac{1}{c\, V_{max}^{b}} + r_f + r_m \left(\frac{A_o}{A_m}\right) + \frac{1}{h_i}\left(\frac{A_o}{A_i}\right) . \qquad (33)$$

Assuming that r_f , r_m, and h_i are constant, this equation reduces to the following form:

$$\frac{1}{U_o} = \frac{1}{c\, V_{max}^{b}} + M , \qquad (34)$$

where

$$M = \text{a constant} = r_f + r_m \left(\frac{A_o}{m}\right) + \frac{1}{h_i}\left(\frac{A_o}{A_i}\right) .$$

A plot of $(1/U_o)$ vs $(1/V_m^b)$ on rectangular coordinates should result in a straight line having a slope of $(1/c)$ and an intercept value of M.

DETERMINATION OF OUTSIDE-AIR FILM COEFFICIENT

The value of the exponent, b, was obtained using a least mean square[22] analysis of the all-aluminum-tube test data. Various exponents were assumed and the deviations of the data from Equation 34 were calculated. The sum of the square of the deviations were plotted vs the assumed exponents as shown in Fig. 10. The best exponent was obtained from the minimum value of the sums of the square of the deviations. As given in Fig. 10, the exponent value obtained using this procedure is 0.4.

Figure 11 presents a plot of $(1/U_o)$ vs $(1/V_m^{0.4})$ for the all-aluminum-tube test data. The solid line given on this figure was obtained using a least mean square fit of the data and has the equation

$$\frac{1}{U_o} = \frac{1}{0.465\, V_m^{0.4}} + 0.00481 . \qquad (35)$$

By comparison of Equation 34 and 35, the values of c and M are obtained as

c = 0.465 and
M = 0.00481.

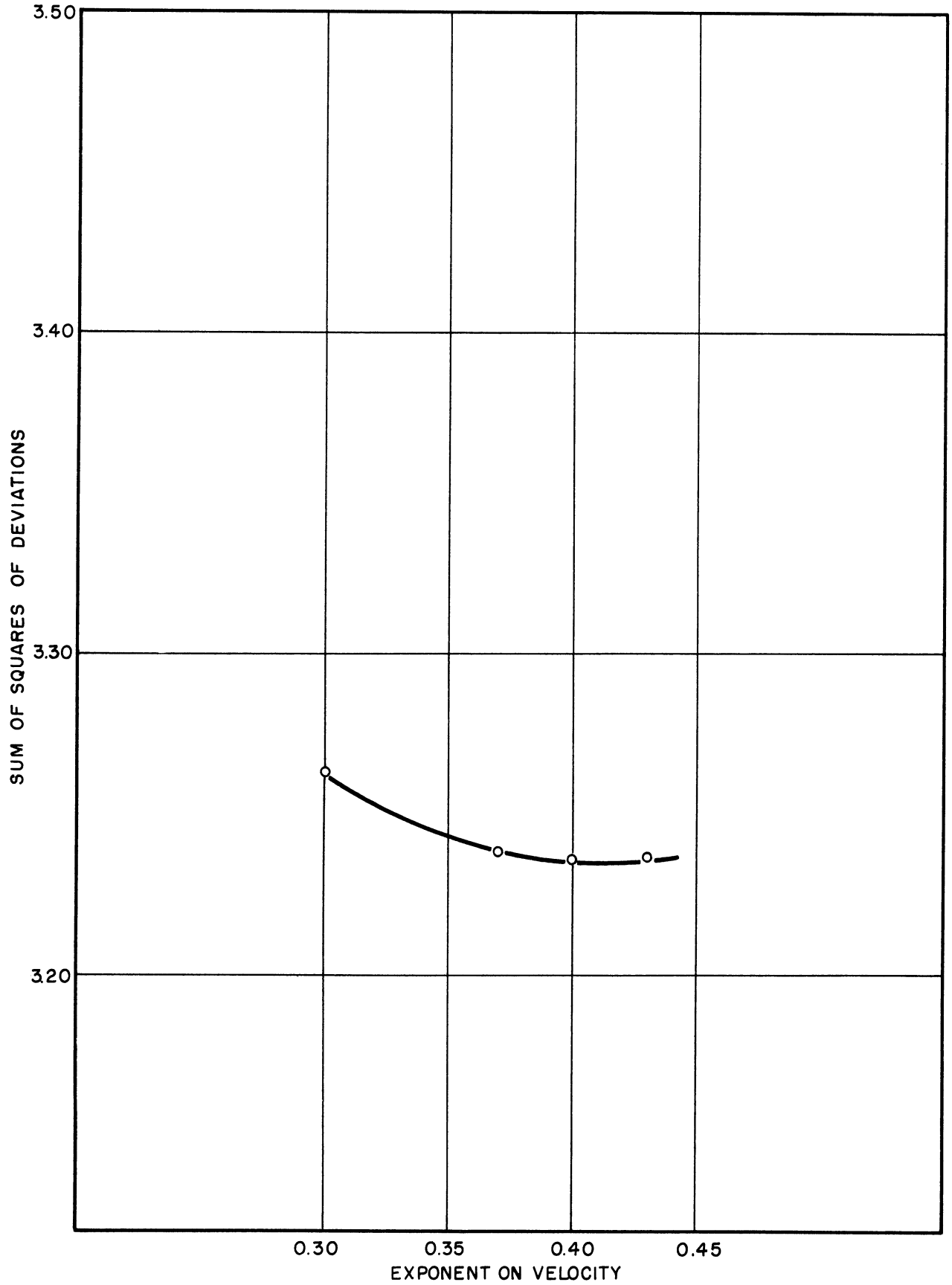

Fig. 10. All-aluminum tubes; determination of exponent on velocity ($h_o = AV_m^b$).

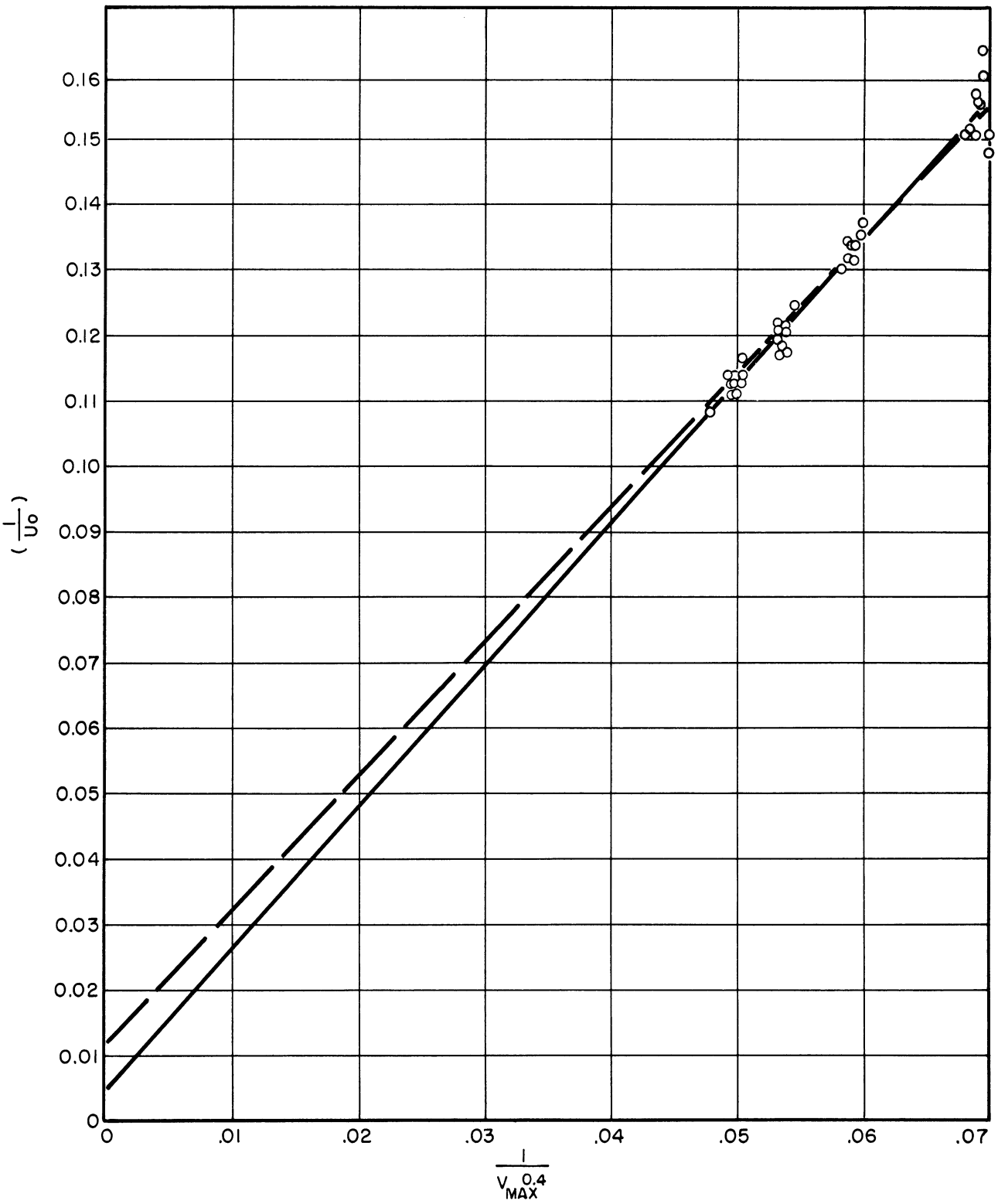

Fig. 11. Wilson plot for all-aluminum-tube data.

The outside-air film coefficient obtained from the above analysis is expressed by the equation

$$h_o' = 0.465\ V_m^{0.4} . \qquad (36)$$

A second least mean square analysis was made on the all-aluminum-tube test data to determine the validity of the assumption of a constant fin resistance. The analysis employed a modified form of Equation 34, of the type

$$\frac{1}{U_o} - r_f = \frac{1}{c'\ V_m^{b'}} + m', \qquad (37)$$

where

c' = a constant,
b' = a constant, and
m' = a constant $= r_m \left(\frac{A_o}{A_m}\right) + \frac{1}{h_i}\left(\frac{A_o}{A_i}\right)$.

The resistance of the fin was determined for each experimental point, using Fig. 4 and Equation 36.

The constants obtained from this analysis were

$$c' = 0.469,$$
$$b' = 0.396, \text{ and}$$
$$m' = -0.0036 .$$

The outside-air film coefficient obtained from this analysis is expressed by the equation

$$h_o' = 0.469\ V_m^{0.396} . \qquad (38)$$

A comparison of Equations 36 and 38 indicates that for all practical purposes the outside-air film coefficients predicted by these equations are identical. Equation 36 is presented graphically in Fig. 12 and will be used throughout this report to predict the air film coefficient for 2-in.-OD finned tubes in the air-test apparatus.

DETERMINATION OF INSIDE STEAM-CONDENSING COEFFICIENT

The inside steam condensing can be calculated from the expression (see Equation 34)

$$\frac{1}{h_i}\left(\frac{A_o}{A_i}\right) = M - \left(r_f + r_m \frac{A_o}{A_i}\right) . \qquad (39)$$

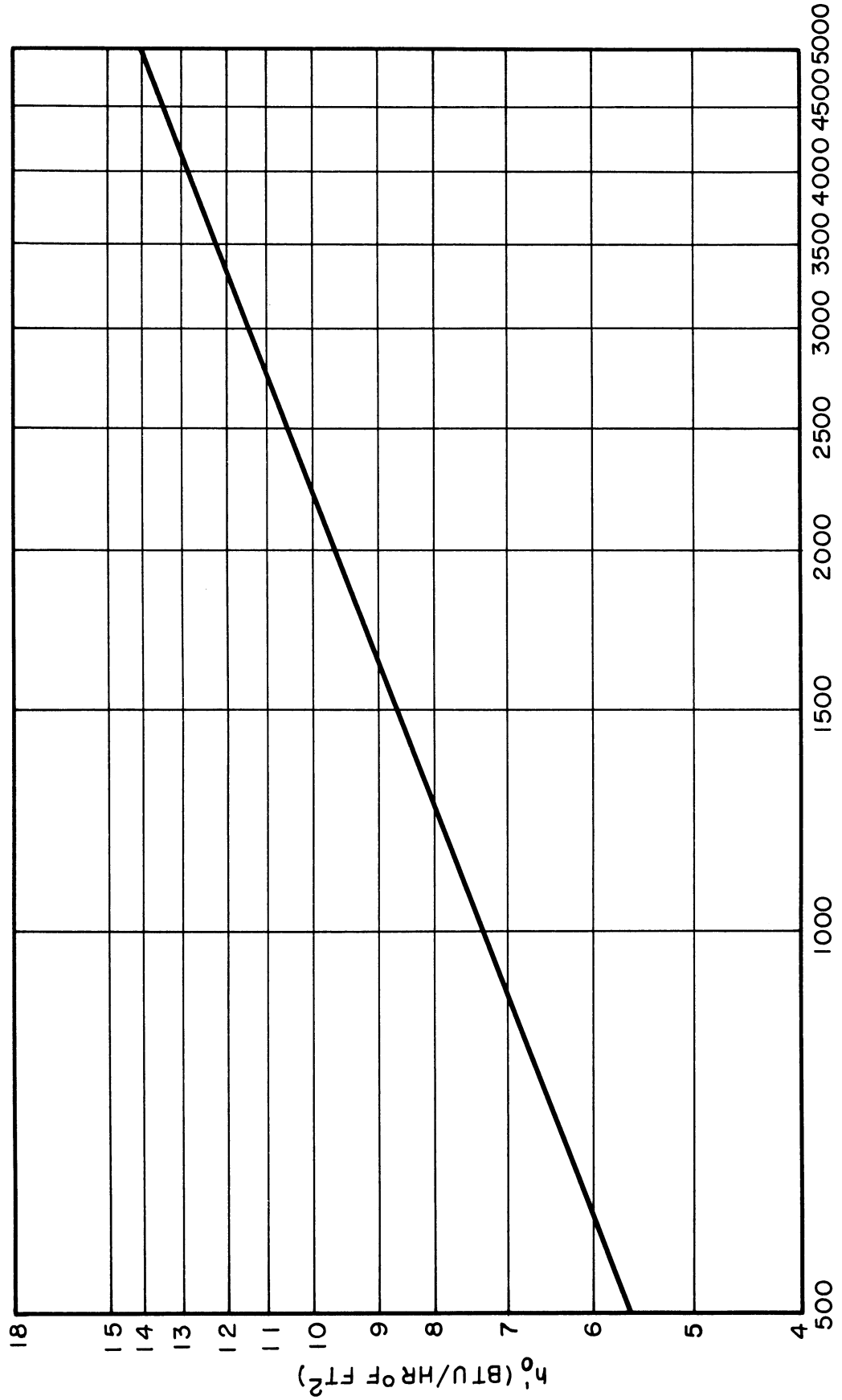

Fig. 12. Air film coefficient as a function of air velocity.

The value of M is given in the previous section as 0.00481. The average fin resistance is obtained from Fig. 4 as $r_f = 0.0072$. The metal resistance is computed as

$$r_m = \frac{X\ A_o}{K\ A_m} , \qquad (40)$$

where

X = average root-wall thickness = 0.078/12 ft,
K = thermal conductivity of metal root wall = 121 Btu/hr/°F/ft, and

$\frac{A_o}{A_m}$ = ratio of outside to mean metal area = 13.2 (dimensionless).

Substituting,

$$r_m = \frac{(.078/12)(13.2)}{121} = 0.00071 \frac{\text{hr/°F/ft}^2\text{(outside)}}{\text{Btu}} .$$

Substituting the values of M, r_f, and r_w (A_o/A_i) into Equation 39, the inside resistance is obtained as

$$\frac{1}{h_i}\left(\frac{A_o}{A_i}\right) = 0.0048 - (0.0072 + 0.00071) = -0.00311 .$$

The above indicates that the inside condensing coefficient, computed from the least mean square fit of the all-aluminum-tube test data, is a negative value. This is not physically possible. The reason for this apparent discrepancy can be seen from examination of Fig. 11. The solid line given on this figure represents Equation 36, obtained from the least mean square fit of the data. The numerical value of M is found from the value of $(1/U_o)$ when $(1/V_m^{0.4})$ is equal to zero. The data used in the analysis and plotted on this figure range from approximately $(1/V_m^{0.4})$ = .049 to $(1/V_m^{0.4})$ = .07. Thus the line representing the data is extrapolated about two and one half times the range of the data in order to obtain the intercept value.

A dashed line is also included in Fig. 11. The intercept of this line has a value of 0.01202 predicted by a steam-condensing coefficient calculated using Nusselt's theoretical equation.[23] As shown on Fig. 11, the dotted line reasonably represents the all-aluminum-tube air-test data. The sensitivity of the air test apparatus is such that the condensing coefficient cannot be experimentally determined.

XII. ANALYSIS OF BIMETAL-TUBE DATA

The overall coefficient of heat transfer with bimetal tubes can be computed using the data given in Appendix F and the modified long-form procedure illustrated in Appendix G. Assuming no fouling present on the tube, the overall coefficient is related to the individual resistances to heat transfer by the relationship

$$\frac{1}{U_o} = \frac{1}{h'_o} + r_f + r_m\left(\frac{A_o}{A_m}\right) + r_b\left(\frac{A_o}{A_L}\right) + \frac{1}{h_i}\left(\frac{A_o}{A_i}\right). \qquad (41)$$

The outside-air film coefficient is a function of only the air mass velocity and the tube and apparatus geometry (for moderate temperature ranges) and is independent of the bond resistance of the tube. Since the exterior geometries of the bimetal and the all-aluminum tubes are essentially the same, the outside-air film coefficient for the bimetal tubes is obtained from the all-aluminum-tube data as

$$h'_o = 0.465\ V_{max}^{0.4}. \qquad (36)$$

Assuming constant fin, steam, and bond resistances and substituting Equation 36 into Equation 41,

$$\frac{1}{U_o} = \frac{1}{0.465\ V_m^{0.4}} + M'', \qquad (42)$$

where

M'' = a constant for any one bimetal tube =

$$r_f + r_m\left(\frac{A_o}{A_m}\right) + r_b\left(\frac{A_o}{A_L}\right) + \frac{1}{h_i}\left(\frac{A_o}{A_i}\right).$$

A comparison of Equations 42 and 34 indicates that they are of the same form and therefore a plot of $(1/U_o)$ vs $(1/V_m^{0.4})$ on rectangular coordinates should also result in a straight line for the bimetal-tube data. A comparison of Equations 42 and 35 further indicates that the data for a bimetal tube plotted in the above manner should result in a straight line which is parallel to that obtained for the all-aluminum tubes, but having a different intercept (M'') value. Assuming that the steam condensing coefficient for a bimetal tube is the same as for an all-aluminum, the difference in intercepts is

$$M'' - M_{(aluminum)} = \left[r_m\left(\frac{A_o}{A_m}\right)_{bimetal} - r_m\left(\frac{A_o}{A_m}\right)_{aluminum}\right] + r_b\left(\frac{A_o}{A_L}\right). \qquad (43)$$

Figure 13 presents a plot of $(1/U_o)$ vs $(1/V_{max}^{0.4})$ for five different bimetal tubes. Superimposed on this figure is the corresponding line obtained from the analysis of the all-aluminum-tube data (see Fig. 11). The bond resistances obtained using the intercept values given in this figure and Equation 43 are calculated in Appendix H and tabulated in Table VI.

TABLE VI

BOND-RESISTANCE VALUES FOR FIVE BIMETAL TUBES
(Copper Liner Material)

Tube No.	Bond Resistance x $(\frac{A_o}{A_L})$	Bond Resistance (based on liner area)
3	.09934	.00725
4	less than 0.0068	less than 0.0005
36	.01004	.000733
54	.01684	.00123
38	.06664	.00485

Bond-resistance values, such as given in Table VI, can be directly substituted into an overall coefficient equation such as Equation 41. Thus the designer can take into account the effect of the bond on the heat transfer performance of a unit in the design of equipment.

A combined heat transfer coefficient which is a function of only the maximum air velocity (for a particular tube in the air test apparatus) can be computed by combining the bond and air film resistances. Figure 14 presents this type of a plot where

$$\left[\frac{1}{\frac{1}{h'_o} + r_b\left(\frac{A_o}{A_L}\right)}\right]$$

is plotted vs the maximum air velocity in feet per minute on logarithmic coordinates. The line corresponding to the outside film coefficient ($r_b = 0$) for this figure was obtained from Equation 36. This figure can be used to predict the effect of the bond resistance on the performance of a tube, as is illustrated in the following example:

A bimetal tube, with no bond resistance, tested in the air-test apparatus at a maximum air velocity of 1500 ft/min would have an outside coefficient h'_o of 8.7. If this perfect tube were replaced by a second bimetal tube having a bond-resistance value of 0.001, the air velocity required to maintain the same overall coefficient would be 2120 ft/min for an increase of 41.4%. If the air velocity for the second tube were maintained

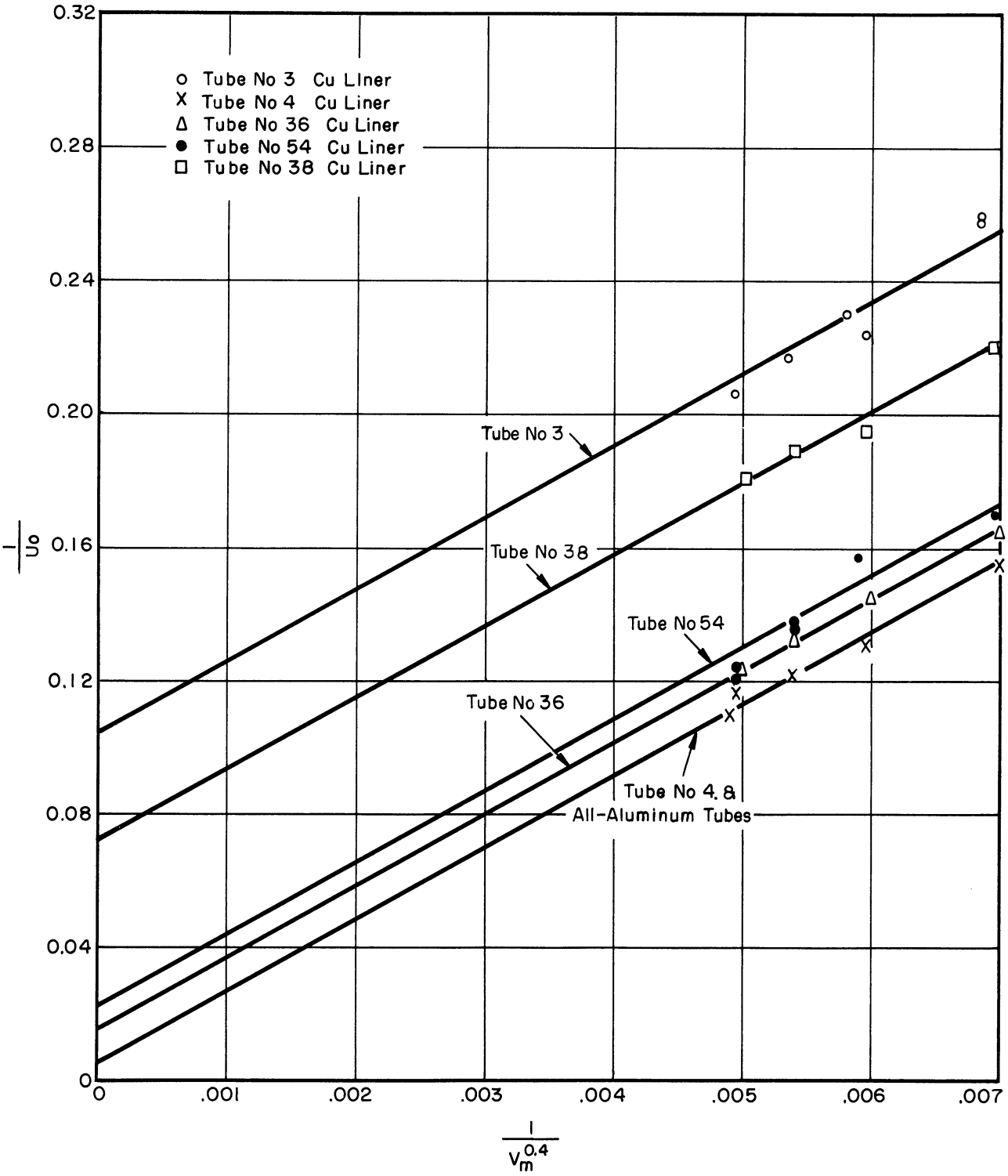

Fig. 13. Wilson plot for bimetallic tubes.

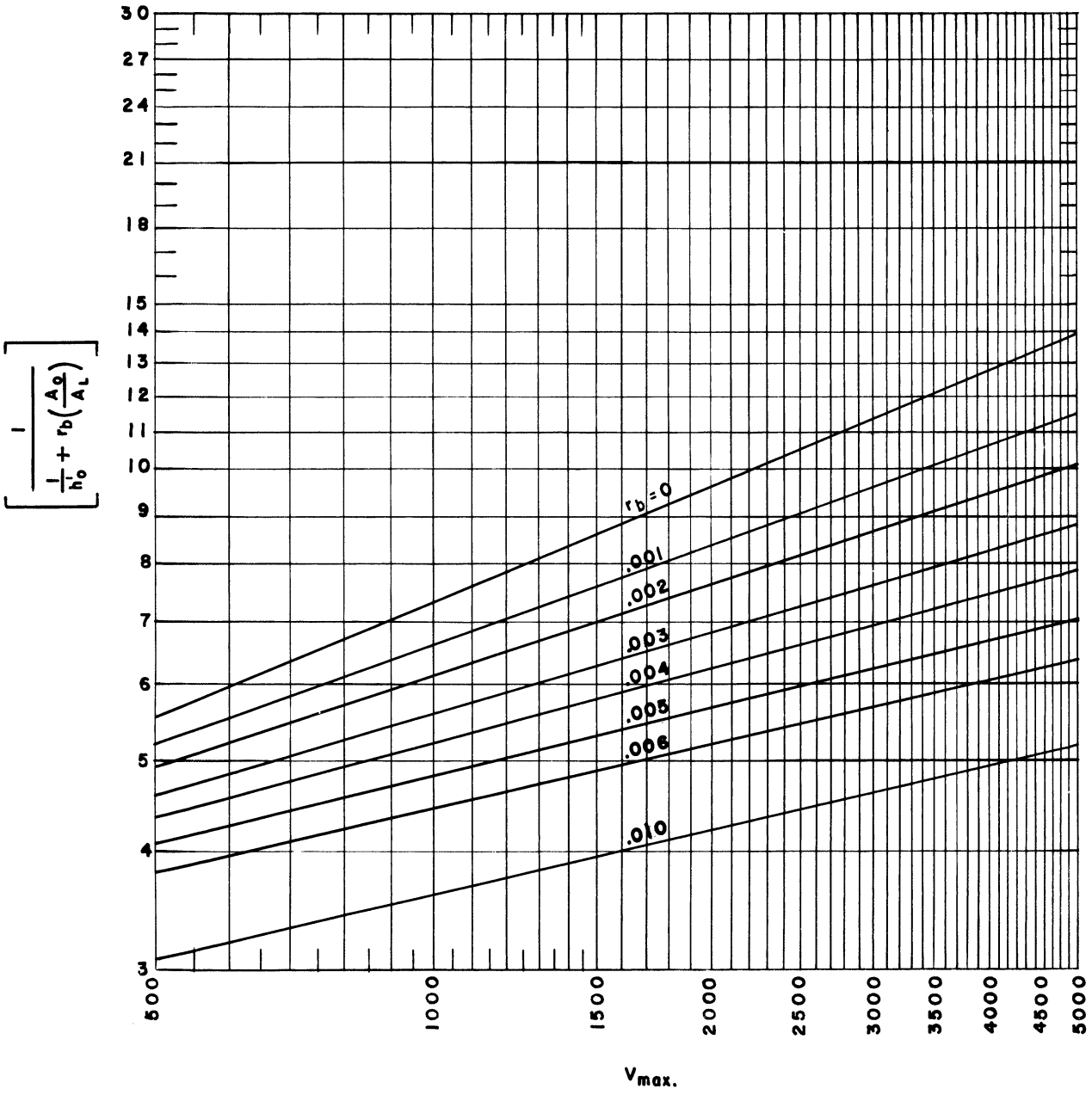

Fig. 14. Combined heat transfer coefficient versus V_{max} for various bond resistances.

at 1500 ft/min, the coefficient would drop to 7.7 for a decrease of 11.5%.

Figure 15 presents the information given in Fig. 44 with the coefficient based upon the tube-liner OD area and the air velocity based upon the face area of the tube. The average outside heat transfer area and minimum flow area used for these conversions were obtained from the nominal dimensions of the tubes tested.

XIII. SENSITIVITY OF AIR-TEST APPARATUS

The sensitivity of the air-test apparatus to bond-resistance differences between bimetal tubes is determined by (1) the degree to which the bond resistance controls the performance of the tubes and (2) the accuracy of the predicted air film, fouling, metal, and steam resistances to heat transfer. This can be illustrated by Fig. 16 where the percent of the heat transfer resistance due to the bond is plotted vs the bond-resistance with parameters of air film coefficients for a 16-gage admiralty tube having an inside coefficient of 1000.

By use of this figure, the limits of the calculated bond-resistance value can be determined if the accuracy of the overall coefficient is also known. This is illustrated in the following two examples.

EXAMPLE 1

It is assumed that an admiralty liner bimetal tube is installed in the air-test apparatus having a calculated bond-resistance value of 0.001 when the steam coefficient is 1000 and the air film coefficient, h_o', is 10. Figure 16 indicates that the bond resistance is 10% of the overall resistance to heat transfer. (All other resistances constitute 90% of the total resistance.) In this range of maximum velocity, the overall coefficient is usually known within $\pm$ 3%. Since the bond resistance is obtained as the difference between the overall resistance and all individual resistances except the bond, the percent of resistance due to the bond is obtained for the limiting coefficients as:

(a) true overall coefficient 3% higher than measured:

$$\text{resistance due to bond} = \left(\frac{103 - 90}{103}\right) 100 = 12.6\% \quad \text{(of overall resistance)}$$

(b) true overall coefficient 3% lower than measured:

$$\text{resistance due to bond} = \left(\frac{97 - 90}{97}\right) 100 = 7.2\% \quad \text{(of overall resistance)}$$

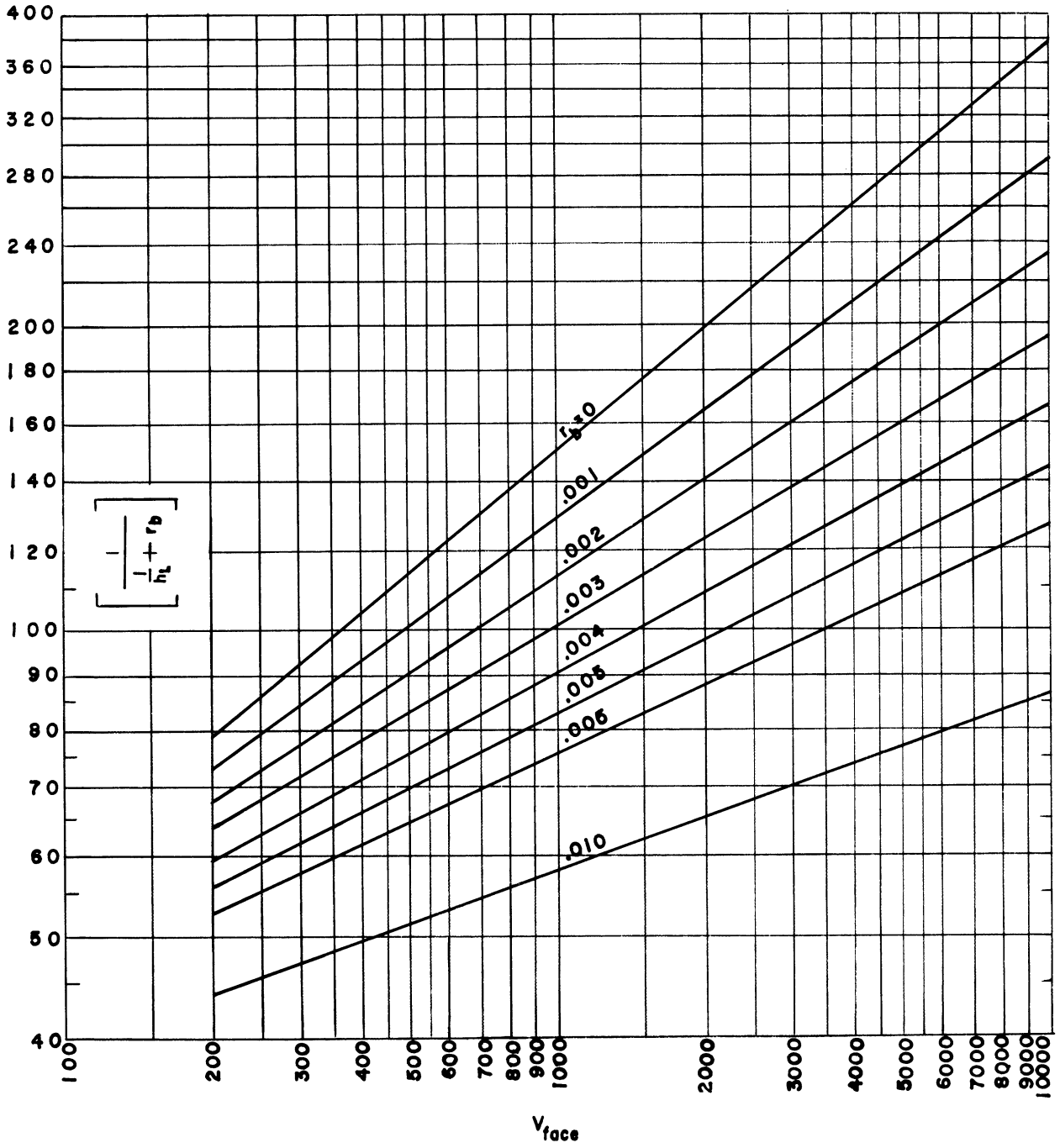

Fig. 15. Combined heat transfer coefficient versus V_{face} for various bond resistances.

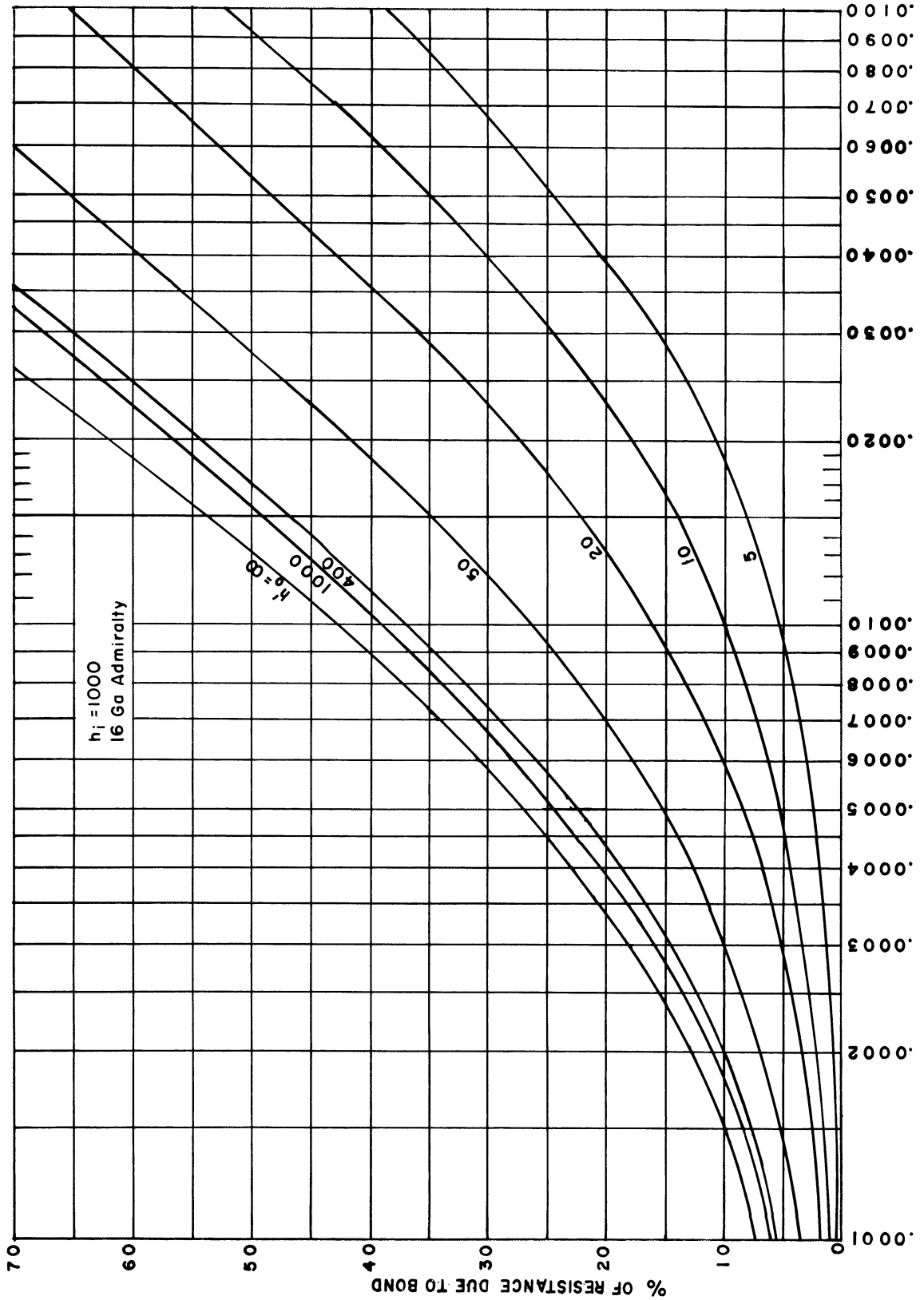

Fig. 16. Percent of resistance due to bond resistance for h_i = 1000.

From Fig. 16, the corresponding bond-resistance values are 0.0013 and 0.00068, respectively. Thus, although the overall coefficient is known within ± 3%, the bond resistance is known only within ± 30%. Uncertainties in the air film and steam condensing coefficients tend to increase the uncertainty in the measured bond-resistance values.

EXAMPLE 2

Assume the same admiralty liner tube is run at a lower air rate such that the outside-air film coefficient, h_o', is 5. The bond-resistance value is again computed as 0.001 (with a steam condensing coefficient of 1000). From Fig. 16, the percent of the total resistance attributable to the bond is 5.5%. Again allowing 3% uncertainty in the overall coefficient, the percent of the resistance due to the bond for the limiting coefficients is:

(a) true overall coefficient 3% higher than measured:

$$\text{resistance due to bond} = \left(\frac{103 - 94.5}{103}\right) 100 = 8.25\%$$

(b) true overall coefficient 3% lower than measured:

$$\text{resistance due to bond} = \left(\frac{97 - 94.5}{97}\right) 100 = 2.58\%.$$

From Fig. 16, the corresponding bond-resistance values are 0.0015 and 0.00053, respectively. Thus, although the overall coefficient is known within ± 3%, the bond resistance is known only within 0.001 ± 0.0005 or ± 50%.

As shown in Fig. 16, the higher the bond resistance the more sensitive the air-test device because the bond resistance represents a higher percentage of the overall resistance for any fixed air film coefficient.

Allowing a 3% indeterminacy in the overall coefficient, the smallest bond resistance measurable with confidence ($h_o' = 10$) would be about 0.00027. The tube in this particular case would have to perform as well as the average of the monometallic tubes (allowing for differences in metal resistance).

Figure 17 presents the same information as Fig. 16 with an inside coefficient of 2000. As seen from a comparison of the two figures, a change in the inside coefficient shifts the position of the resulting curves. The measurable bond resistance is still in the order of 0.00027.

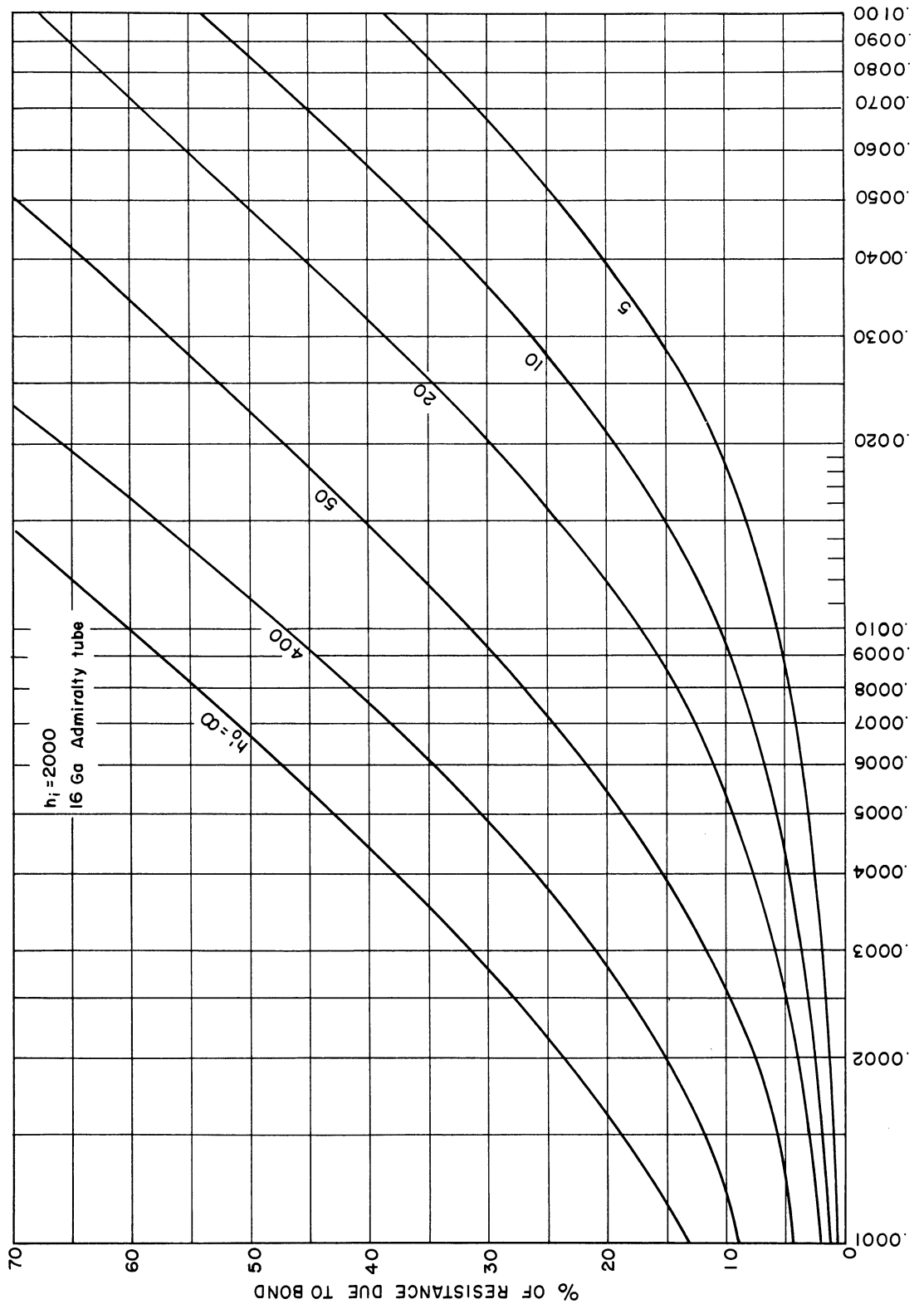

Fig. 17. Percent of resistance due to bond resistance for h_i = 2000.

XIV. CONCLUSIONS AND RECOMMENDATIONS

The following conclusions and recommendations are made:

A. The single-tube test data (i.e., Equation 36 for air film coefficient) cannot be used for the design of tube banks.

B. The effect of the bond resistance (interfacial contact resistance) should be included in the design calculations as an added resistance to heat transfer for design purposes.

C. The bond resistance with steam condensing inside bimetal tubes and with average air temperatures of 110°F is about 0.001 (based on liner area) for an acceptable bimetal tube.

D. The equipment can be used for production control if the accuracy indicated is acceptable ($0.001 \pm .0003$ at $h_o' = 10$).

E. The equipment cannot be used to obtain sufficiently accurate bond-resistance values in the cyclic testing of bimetal tubes.

F. The air-test apparatus when used for production control should be operated at the highest air throughput with screens in order to obtain the greatest sensitivity to bond resistance.

G. A bond-resistance testing apparatus that can accurately measure bond resistance of the order of 0.0004 ± 0.0001 or less is seriously needed. We believe that bimetal tubes can be consistently fabricated without serious losses for shipment with bond resistance not exceeding 0.0005 if a sensitive production-control device is available.

H. The bond resistance value of 0.001 as given in C and D above amounts to approximately 10% of the total resistance to heat transfer in normal applications. It is recommended that the control value be reduced to at least 5% (or to 0.0005).

REFERENCES

1. W. H. McAdams. Heat Transmission, Third Edition. New York: McGraw-Hill Book Co., 1954, pp. 17-18.

2. N. D. Weills and E. A. Ryder, "Thermal Resistance Measurements of Joints Formed Between Stationary Metal Surfaces," Trans. ASME, 71:259 (1949).

3. F. Kesselring. Elements of Switchgear Design. New York: Pitman Pub. Corp., 1932.

4. R. Jacobs and C. Starr, "Thermal Conductance of Metallic Contacts," Rev. Sci. Inst., 10:140 (1939).

5. F. P. Bowden and D. Tabor, "The Area of Contact Between Stationary and Between Moving Surfaces," Proc. Roy. Soc. London, A, 169:391-413 (1939).

6. T. N. Centinkale and M. Fishenden, "Thermal Conductance of Metal Surfaces in Contact," Proceedings of the General Discussion on Heat Transfer, Section II, Institute of Mechanical Engineering and ASME, London, 1951.

7. R. Holm. Electrical Contacts. Stockholm: Hugo Gebers Forlag, 1946.

8. A. E. H. Love. A Treatise on the Mathematical Theory of Elasticity. New York: Dover Publications, 1944, p. 196.

9. W. B. Kouwenhoven and J. H. Potter, "Thermal Resistance of Metal Contacts," The Welding Journal (Research Supplement), 27:515-S (1948).

10. A. W. Brunot and F. F. Buckland, "Thermal Contact Resistance of Laminated and Machined Joints," Trans. ASME, 71:253 (1949).

11. W. H. Carrier and S. W. Anderson, "The Resistance to Heat Flow Through Finned Tubing," Heating, Piping, and Air Conditioning, May, 1944, pp. 304-318.

12. Air Conditioning Refrigerating Data Book, Design, American Society of Refrigerating Engineers, 9th Ed., 1955.

REFERENCES (Concl.)

13. K. A. Gorden, "The Efficiency of Extended Surface," Trans. ASME, 65: 621-623 (1945).

14. R. H. Norris and W. A. Spofford, "High Performance Fins for Heat Transfer," Trans. ASME, 64:489-496 (1942).

15. A. W. Lemmon, Jr., A. P. Colburn, and H. B. Nottage, "Heat Transfer from a Baffled-Finned Cylinder to Air," Trans. ASME, 67:601 (1945).

16. S. L. Jameson, "Tube Spacing in Finned Tube Banks," Trans. ASME, 67:633 (1945).

17. W. M. Kays and A. C. London. Compact Heat Exchange Surfaces. Palo Alto, California: The National Press, 1955.

18. D. L. Katz, K. O. Beatty, Jr., and A. S. Foust, "Heat Transfer Through Tubes with Integral Spiral Fins," Trans. ASME, 67:665 (1945).

19. T. E. Schmidt, "Heat Transmission and Pressure Drop in Banks of Finned Tubes and in Laminated Coolers," Proceedings of the General Discussion on Heat Transfer, Section II, Institute of Mechanical Engineering and ASME, London, 1951, p. 186.

20. D. L. Katz, E. H. Young, et al., "Correlation of Heat Transfer and Pressure Drop for Air Flowing Across Banks of Finned Tubes," Report 30, Project 1592, Eng. Res. Inst., Univ. of Mich., 1954.

21. E. H. Young, et al., "Investigation of the Performance of Vane-Type Anemometers in a Four-Inch Duct," Report 37, Project 1592, Eng. Res. Inst., Univ. of Mich., 1955.

22. W. J. Youden. Statistical Methods for Chemists. New York: John Wiley and Sons, 1951, pp. 40-49.

23. W. H. McAdams. Op. cit., p. 338, Equation (13-12).

APPENDIX A

DERIVATION OF FIN RESISTANCE METHOD
FOR A FOULED TUBE

Nomenclature

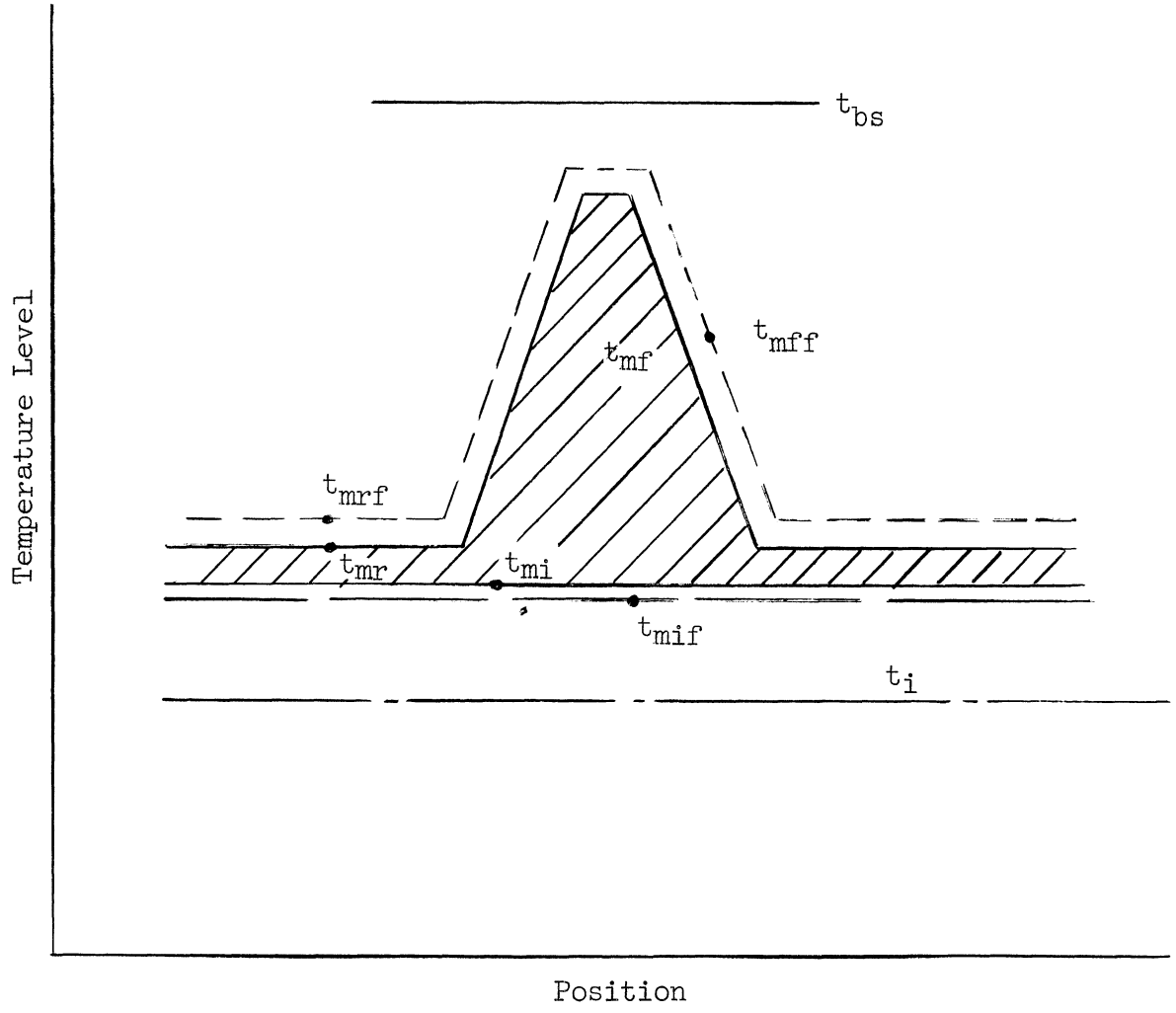

Let the coefficient be constant for both root and fin area and equal to h'_o and let the outside fouling resistance be constant and equal to r'_o.

Ignoring the outside area difference due to fouling, the heat transfer to the root portion of the tube is

$$q_r = h'_o A_r (t_{bs} - t_{mrf}) . \quad (1A)$$

It necessarily follows that

$$q_r = \left(\frac{1}{r'_o}\right) A_r (t_{mrf} - t_{mr}) . \quad (2A)$$

Solving Equation 2A for t_{mrf} gives

$$t_{mrf} = \frac{r'_o q_r}{A_r} + t_{mr} . \quad (3A)$$

Substituting Equation 3A into Equation 1A gives

$$q_r = h'_o A_r \left(t_{bs} - \frac{r'_o q_r}{A_r} - t_{mr}\right). \quad (4A)$$

Rearranging Equation 4A gives

$$q_r = \frac{A_r}{\frac{1}{h'_o} + r'_o} (t_{bs} - t_{mr}). \quad (5A)$$

Now, again ignoring the area difference due to fouling, the heat transfer to the fin is given by

$$q_f = h'_o A_f (t_{bs} - t_{mff}), \quad (6A)$$

and it also follows that

$$q_f = \frac{1}{r'_o} A_f (t_{mff} - t_{mf}), \quad (7A)$$

where t_{mff} and t_{mf} are the integrated average fouled-fin interface and fin-metal interface temperatures, respectively. Solving Equation 7A for t_{mff},

$$t_{mff} = \frac{r'_o q_f}{A_f} + t_{mf}. \quad (8A)$$

Substituting Equation 8A into Equation 6A gives

$$q_f = h'_o A_f \left(t_{bs} - \frac{r'_o q_f}{A_f} - t_{mf}\right). \quad (9A)$$

Rearranging Equation 9A gives

$$q_f = \frac{A_f}{\frac{1}{h'_o} + r'_o} (t_{bs} - t_{mf}). \quad (10A)$$

Equation 10A for the fin is analogous to Equation 5A for the root. Now, the total heat transfer through the tube must equal the sum of that occurring across the root wall and that occurring across the finned section, or

$$q_T = q_r + q_f, \quad (11A)$$

where q_T = total heat transfer rate.

Substituting Equations 5A and 10A into Equation 11A gives

$$q_T = \frac{A_r}{\left(\frac{1}{h'_o} + r'_o\right)} (t_{bs} - t_{mr}) + \frac{A_f}{\left(\frac{1}{h'_o} + r'_o\right)} (t_{bs} - t_{mf}). \quad (12A)$$

Now, defining a factor equal to the ratio of the temperature drop from the bulk stream to the fin and the drop from the bulk stream to the root, i.e., fin efficiency,

$$E_f = \frac{t_{bs} - t_{mf}}{t_{bs} - t_{mr}}. \quad (13A)$$

Substituting Equation 13A into Equation 12A gives

$$q_T = \frac{A_r}{\left(\frac{1}{h'_o} + r'_o\right)} (t_{bs} - t_{mr}) + \frac{A_f}{\left(\frac{1}{h'_o} + r'_o\right)} (t_{bs} - t_{mr}) E_f. \quad (14A)$$

Rearranging Equation 14A gives

$$q_T = \frac{(t_{bs} - t_{mr})}{\left(\frac{1}{h'_o} + r'_o\right)} [A_r + E_f A_f]. \quad (15A)$$

Defining an equivalent area as

$$Aeq = A_r + E_f A_f, \quad (16A)$$

substituting Equation 16A into Equation 15A gives

$$q_T = \frac{1}{\left(\frac{1}{h_o'} + r_o'\right)} Aeq\ (t_{bs} - t_{mr}). \qquad (17A)$$

Now, the remainder of the heat transfer coefficients, involved have the relationship

$$q_T = \frac{A_m}{r_m}(t_{mr} - t_{mi}) = \frac{A_i}{r_i}(t_{mi} - t_{mif}) = A_i\, h_i\, (t_{mif} - t_i), \qquad (18A)$$

where A_m = the mean metal heat transfer area,

A_i = the inside heat transfer area,

$\frac{x}{k} = r_m$ = the metal resistance to heat transfer,

r_i = the inside fouling resistance to heat transfer,

h_i = the inside film coefficient for heat transfer,

t_{mi} = the inside tube-metal temperature,

t_{mif} = the inside fouling-film interface temperature, and

t_i = the bulk stream inside temperature.

Upon solving Equation 18A for the interface temperature as in the outer films, the following can be obtained:

$$q_T = \left[\frac{1}{\frac{1}{h_i} + r_i + \frac{r_m A_i}{A_m}}\right] A_i\ (t_{mr} - t_i). \qquad (19A)$$

Solving Equation 17A for t_{mr},

$$t_{mr} = t_{bs} - \frac{q_T\left(\frac{1}{h_o'} + r_o'\right)}{Aeq}. \qquad (20A)$$

Substituting Equation 20A into Equation 19A gives

$$q_T = \left[\frac{1}{\frac{1}{h_i} + r_i + r_m \frac{A_i}{A_m}}\right] A_i \left[t_{bs} - \frac{q_T\left(\frac{1}{h_o'} + r_o'\right)}{Aeq} - t_i\right]. \qquad (21A)$$

Rearranging Equation 21A gives

$$q_T = \frac{Aeq\,[t_{bs} - t_i]}{\left(\frac{Aeq}{A_i}\right)\frac{1}{h_i} + \left(\frac{Aeq}{A_i}\right) r_i + \frac{Aeq}{A_m} r_m + \frac{1}{h'_o} + r'_o} \quad . \tag{22A}$$

Now, defining

$$Ueq = \frac{q_T}{Aeq\,(t_{bs} - t_i)} \,, \tag{23A}$$

solving Equation 23A for q_T and substituting into Equation 22A gives

$$Ueq = \frac{1}{\frac{Aeq}{A_i}\frac{1}{h_i} + \frac{Aeq}{A_i} r_i + \frac{Aeq}{A_m} r_m + \frac{1}{h'_o} + r'_o} \quad . \tag{24A}$$

Now, defining

$$U_o = Ueq\left(\frac{Aeq}{A_o}\right), \tag{25A}$$

substituting Equation 25A into Equation 24A and solving for U_o gives

$$U_o = \frac{\frac{Aeq}{A_o}}{\left(\frac{Aeq}{A_i}\right)\frac{1}{h_i} + \left(\frac{Aeq}{A_i}\right) r_i + \left(\frac{Aeq}{A_m}\right) r_m + \frac{1}{h'_o} + r'_o} \quad . \tag{26A}$$

Solving Equation 26A for $1/U_o$ gives

$$\frac{1}{U_o} = \left(\frac{A_o}{A_i}\right)\frac{1}{h_i} + \left(\frac{A_o}{A_i}\right) r_i + \left(\frac{A_o}{A_m}\right) r_m + \frac{A_o}{Aeq}\left(\frac{1}{h'_o}\right) + \left(\frac{A_o}{Aeq}\right) r'_o \quad . \tag{27A}$$

Defining an overall resistance containing a fin-metal resistance, r_f,

$$\frac{1}{U_o} = \left(\frac{A_o}{A_i}\right)\frac{1}{h_i} + \left(\frac{A_o}{A_i}\right) r_i + \left(\frac{A_o}{A_m}\right) r_m + r_f + \frac{1}{h'_o} + r'_o \quad . \tag{28A}$$

Setting the right-hand sides of Equation 28A equal to Equation 27A and canceling terms gives

$$r_f + \frac{1}{h'_o} + r'_o = \frac{A_o}{Aeq}\left(\frac{1}{h'_o}\right) + \frac{A_o}{Aeq} r'_o \quad . \tag{29A}$$

Solving Equation 29A for r_f and simplifying gives

$$r_f = \left[\frac{1}{h'_o} + r'_o\right]\left[\frac{A_o - Aeq}{Aeq}\right], \tag{30A}$$

but

$$A_o = A_r + A_f \tag{31A}$$

and

$$Aeq = A_r + E_f A_f . \tag{32A}$$

Substituting Equations 31A and 32A into Equation 30A and rearranging gives

$$r_f = \left[\frac{1}{h'_o} + r'_o\right]\left[\frac{1 - E_f}{\frac{A_r}{A_f} + E_f}\right] . \tag{33A}$$

APPENDIX B

ANEMOMETER CORRECTION FACTOR OBTAINED FROM THE AIR-TEST APPARATUS

DATA AND CALCULATED RESULTS FOR ANEMOMETER CORRECTION FACTOR

Run No.	Ambient Press (mm Hg)	Ambient Temp (°C)	Steam Press (psig)	Steam Temp (°C)	Anemometer Reading (std ft/min)	Inlet-Air Temp (°C)	Outlet-Air Temp (°C)	Condensate Collected (grams)	Time (min)	Heat Transferred (Btu/hr)	Actual Air Velocity (std ft/min)	$\frac{V_{anemometer}}{V_{actual}}$	Remarks
391	737.5	21.0	10.0	114.5	--	--	--	53	15	461	--	--	Calibration of equipment for heat losses.
392	737.5	21.0	10.0	114.5	--	--	--	49	15	424	--	--	
393	737.5	21.0	10.0	114.5	--	--	--	51	15	441	--	--	
394	737.5	21.0	10.0	114.4	--	--	--	49	15	424	--	--	
395	737.5	21.0	10.0	114.5	--	--	--	52	15	450	--	--	
396	737.5	21.0	10.0	114.3	--	--	--	55	15	476	--	--	
397	737.5	21.0	10.0	114.4	1980	25.84	45.60	543	15	4690	1263	1.515	
398	737.5	21.0	10.0	114.3	1919	25.75	45.65	548	15	4730	1283	1.493	
399	731.8	21.5	10.0	114.2	2004	25.65	45.16	556	15	4750	1313	1.528	
400	731.8	21.5	10.0	114.2	2004	25.67	45.26	555	15	4800	1320	1.520	
401	731.8	21.5	10.0	114.5	1643	25.63	47.53	511	15	4410	1071	1.533	
402	731.8	21.5	10.0	114.5	1637	25.64	47.52	513	15	4435	1070	1.528	
403	731.8	21.5	10.0	114.1	1284	26.04	51.11	463	15	4000	840	1.540	
404	731.8	21.5	10.0	114.0	1285	26.14	51.07	466	15	4020	850	1.510	
405	731.8	21.5	10.0	114.1	926	26.06	57.04	400	15	3450	570	1.625	
406	731.8	21.5	10.0	114.2	928	26.04	57.35	398	15	3440	571	1.622	

APPENDIX C

DATA FOR THERMOMETER CORRECTION FACTORS

TEMPERATURE RISE OF INLET AIR DUE TO BLOWER, RADIATION, AND OTHER EFFECTS

Run No.	Ambient-Air Temperature*, °C	Inlet-Air Temperature, °C	$T_{inlet} - T_{ambient}$, °C	V_{max}	Remarks
		Temperature Rise Due to Blower			
437	23.42	24.08	0.66	750	No steam
438	23.07	23.67	0.60	1079	No steam
439	23.07	24.02	0.95	1362	No steam
440	23.04	24.01	1.03	1352	No steam
441	23.38	24.13	0.75	1352	No steam
442	26.35	26.51	0.16	1344	No steam
443	26.46	26.49	0.03	1641	No steam
444	26.48	26.67	0.19	1045	No steam
445	26.08	26.44	0.36	700	No steam
450	26.71	26.90	0.19	1788	No steam
451	26.87	27.12	0.25	1451	No steam
452	26.92	27.24	0.32	1345	No steam
453	28.57	28.93	0.36	960	No steam
		Temperature Rise Due to Blower, Radiation, and Other Effects			
407	27.40	29.55	2.15	748	Steam in tube
408	27.36	29.62	2.26	793	Steam in tube
411	25.67	27.14	1.47	1170	Steam in tube
412	25.72	27.24	1.52	1178	Steam in tube
413	25.51	26.91	1.40	1510	Steam in tube
414	25.68	26.97	1.29	1505	Steam in tube
415	25.82	26.95	1.13	1743	Steam in tube
416	25.80	26.94	1.14	1743	Steam in tube
417	25.94	26.91	0.97	1833	Steam in tube
418	25.95	26.95	1.00	1833	Steam in tube
419	27.83	28.88	1.05	1882	Steam in tube
420	27.73	28.80	1.07	1882	Steam in tube
421	28.06	29.88	1.82	810	Steam in tube
422	28.00	29.92	1.92	810	Steam in tube
423	27.97	29.52	1.55	1213	Steam in tube
424	28.01	29.52	1.51	1213	Steam in tube
425	28.18	29.45	1.27	1215	Steam in tube
426	28.06	29.42	1.36	1213	Steam in tube
427	28.19	29.92	1.73	807	Steam in tube
428	28.32	29.95	1.63	807	Steam in tube
429	28.23	28.92	0.69	1855	Steam in tube
430	28.15	28.91	.76	1855	Steam in tube
431	27.55	28.65	1.10	1886	Steam in tube
432	27.63	28.54	0.91	1886	Steam in tube
433	27.91	29.30	1.39	1220	Steam in tube
434	27.87	29.28	1.41	1225	Steam in tube
435	28.17	30.11	1.94	813	Steam in tube
436	28.18	30.17	1.99	813	Steam in tube

*The ambient-air temperature was measured with a thermometer located at the inlet of the blower.

APPENDIX D

DATA ON EFFECT OF SCREENS

DATA ON EFFECT OF SCREENS

Run No.	Tube Designation	Tube Characteristics	Steam Pressure (Corrected, psia)	Steam Temperature (°F)	Air-Inlet Temperature (Corrected °F)	Air-Outlet Temperature (Corrected °F)	Q (Btu/hr)	ΔT_{LM}	V_{max}	U_o	Orifice Size (in.)	Remarks
					First Tests							
407	17	A_o = 3.63 ft²	24.58	239.25	83.40	137.10	2690	127.30	748	5.60	2	two screens
408	17	A_{flow} = 0.063 ft²	24.58	239.25	83.50	137.38	2870	127.30	793	6.21	2	two screens
411	17	All-aluminum tube	24.50	239.05	79.05	124.65	3570	135.70	1170	7.24	2-1/2	two screens
412	17		24.50	239.05	79.22	124.90	3570	136.60	1178	7.20	2-1/2	two screens
413	17		24.50	239.05	78.65	119.47	4150	138.60	1510	8.24	3	two screens
414	17		24.50	239.05	78.75	119.55	4130	138.60	1505	8.19	3	two screens
415	17		24.50	239.05	78.70	117.00	4475	139.80	1743	8.83	3-1/2	two screens
416	17		24.50	239.05	78.68	116.98	4475	139.60	1743	8.83	3-1/2	two screens
417	17		24.50	239.05	78.65	116.22	4610	140.60	1833	9.02	4	two screens
418	17		24.50	239.05	78.70	116.25	4610	139.60	1833	9.02	4	two screens
419	17		24.50	239.05	82.18	119.12	4660	137.30	1882	9.34	4	one screen
420	17		24.50	239.05	82.05	119.10	4660	137.20	1882	9.34	4	one screen
421	17		24.50	239.05	84.00	141.10	3100	124.10	810	6.88	2	one screen
422	17		24.50	239.05	84.05	141.30	3105	123.80	810	6.91	2	one screen
423	17		24.50	239.05	83.35	129.58	3760	131.50	1213	7.87	2-1/2	one screen
424	17		24.50	239.05	83.35	129.53	3760	131.30	1213	7.89	2-1/2	one screen
425	17		24.50	239.05	83.20	131.70	3950	130.30	1215	8.35	2-1/2	no screen
426	17		24.50	239.05	83.15	131.85	3960	130.10	1213	8.37	2-1/2	no screen
427	17		24.50	239.05	84.05	141.92	3130	123.70	807	6.98	2	no screen
428	17		24.50	239.05	84.10	142.45	3150	123.40	807	7.02	2	no screen
429	17		24.50	239.05	82.25	121.00	4820	137.50	1855	9.65	4	no screen
430	17		24.50	239.05	82.25	121.07	4830	137.50	1855	9.68	4	no screen
431	17		24.50	239.05	81.75	118.95	4710	136.90	1886	9.46	4	one screen
432	17		24.50	239.05	81.56	118.97	4730	140.50	1886	9.28	4	one screen
433	17		24.50	239.05	82.95	129.38	3790	131.20	1220	7.96	2-1/2	one screen
434	17		24.50	239.05	82.90	129.65	3840	131.20	1225	8.07	2-1/2	one screen
435	17		24.50	239.05	84.40	141.80	3130	123.50	813	7.18	2	one screen
436	17		24.50	239.05	84.50	142.30	3170	123.00	813	7.12	2	one screen
					Second Tests							
521	16	A_o = 3.52 ft²	24.31	238.55	77.00	113.90	4570	142.00	1820	9.15	4	two screens
522	16	A_{flow} = 0.0642 ft²	24.31	238.55	81.85	118.10	4420	138.00	1783	9.10	4	one screen
523	16	All-aluminum tube	24.31	238.55	83.00	122.95	3990	134.50	1460	8.42	3	one screen
524	16		24.31	238.55	83.75	129.25	3620	131.20	1165	7.85	2-1/2	one screen
525	16		24.31	238.55	84.20	140.25	2930	124.20	780	6.70	2	one screen
526	16		24.31	238.55	84.85	145.00	3210	121.50	782	7.50	2	no screen
527	16		24.31	238.55	83.27	131.07	3805	129.80	1168	8.34	2-1/2	no screen
528	16		24.31	238.55	82.40	124.67	4480	133.70	1551	9.52	3	no screen

APPENDIX E

SUMMARY OF ALL-ALUMINUM TUBE DATA

SUMMARY OF ALL-ALUMINUM-TUBE DATA

Run No.	Tube Designation	Tube Characteristics	Steam Pressure (Corrected, psia)	Steam Temperature (°F)	Air-Inlet Temperature (Corrected °F)	Air-Outlet Temperature (Corrected °F)	Q (Btu/hr)	ΔT_{LM}	V_{max}	U_o	Orifice Size (in.)
486	21	$A_o = 3.28$ ft^2	24.17	238.35	87.45	143.55	3040	121.00	762	6.65	2
487	21	$A_{flow} = 0.0669$ ft^2	24.17	238.35	86.75	131.98	3420	127.80	1130	7.27	2-1/2
488	21		24.17	238.35	86.37	126.10	4010	132.00	1415	8.05	3
489	21		24.17	238.35	85.50	121.15	4380	134.50	1730	8.60	4
490	22	$A_o = 3.57$ ft^2	24.32	238.60	84.55	120.00	4275	135.00	1775	8.88	4
491	22	$A_{flow} = 0.0638$ ft^2	24.32	238.60	84.90	124.35	3930	133.30	1468	8.25	3
492	22		24.32	238.60	85.07	129.57	3490	130.80	1157	7.47	2-1/2
493	22		24.32	238.60	85.55	140.00	2870	124.00	775	6.48	2
446	16	$A_o = 3.52$ ft^2	24.43	238.88	81.55	136.19	2945	128.20	781	6.26	2
447	16	$A_{flow} = 0.0642$ ft^2	24.43	238.88	81.78	136.36	2900	127.50	779	6.12	2
448	16		24.43	238.88	80.36	117.67	4530	139.80	1785	8.85	4
449	16		24.43	238.88	80.37	117.40	4510	139.70	1785	8.81	4
454	16		24.35	238.68	84.05	138.37	2950	125.20	792	6.43	2
455	16		24.35	238.68	83.70	138.66	2962	125.30	792	6.45	2
456	16		24.35	238.68	82.03	118.60	4430	138.00	1780	8.75	4
457	16		24.35	238.68	82.09	118.60	4410	138.30	1772	8.71	4
458	16		24.12	238.10	81.80	118.42	4430	136.00	1775	8.89	4
459	16		24.12	238.10	81.23	121.88	4100	136.10	1480	8.22	3
460	16		24.12	238.10	79.56	125.90	3675	134.90	1165	7.46	2-1/2
461	16		24.12	238.10	81.95	137.40	2980	126.70	787	6.43	2
462	16		23.94	237.65	80.30	136.40	2980	127.20	792	6.42	2
463	16		23.94	237.65	79.50	126.45	3580	133.50	1132	7.38	2-1/2
464	16		23.94	237.65	79.07	120.75	4100	135.50	1465	8.31	3
465	16		23.94	237.65	79.35	117.05	4510	137.50	1172	9.01	4
478	16		24.11	238.10	83.15	128.85	3590	131.10	1176	7.64	2-1/2
479	16		24.11	238.10	84.20	139.73	2950	124.00	796	6.64	2
480	16		24.11	238.10	82.80	123.68	4030	133.30	1479	8.43	3
481	16		24.11	238.10	82.50	119.65	4430	135.50	1790	9.13	4
482	16		24.25	238.42	85.47	121.80	4260	133.80	1710	8.90	4
483	16		24.25	238.42	85.20	125.70	4020	130.20	1480	8.60	3
484	16		24.25	238.42	85.75	131.35	3540	129.50	1160	7.64	2-1/2
485	16		24.25	238.42	86.75	141.52	2895	121.70	792	6.84	2
521	16		24.31	238.55	77.00	113.90	4570	142.00	1820	9.15	4
466	32	$A_o = 3.365$ ft^2	23.94	237.65	80.15	114.55	4150	139.90	1835	8.83	4
467	32	$A_{flow} = 0.0616$ ft^2	23.94	237.65	80.43	118.60	3795	137.50	1513	8.20	3
468	32		23.94	237.65	81.20	124.45	3365	134.30	1185	7.44	2-1/2
469	32		23.94	237.65	82.65	135.56	2825	127.00	814	6.60	2
470	32		23.94	237.65	82.48	116.62	4100	137.50	1825	8.85	4
471	33	$A_o = 3.43$ ft^2	23.94	237.65	82.05	118.16	4200	137.50	1810	8.90	4
472	33	$A_{flow} = 0.0604$ ft^2	23.94	237.65	82.38	121.99	3860	134.20	1512	8.38	3
473	33		23.94	237.65	83.17	127.63	3445	130.70	1210	7.70	2-1/2
474	33		23.94	237.65	84.51	138.65	2840	124.30	818	6.65	2
407	17	$A_o = 3.63$ ft^2	24.58	239.25	83.40	137.10	2690	127.30	748	5.60	2
408	17	$A_{flow} = 0.063$ ft^2	24.58	239.25	83.50	137.38	2870	127.30	793	6.21	2
411	17		24.50	239.05	79.05	124.65	3570	135.70	1170	7.24	2-1/2
412	17		24.50	239.05	79.22	124.90	3570	136.60	1178	7.20	2-1/2
413	17		24.50	239.05	78.65	119.47	4150	138.60	1510	8.24	3
414	17		24.50	239.05	78.75	119.55	4130	138.60	1505	8.19	3
415	17		24.50	239.05	78.70	117.00	4475	139.80	1743	8.83	3-1/2
416	17		24.50	239.05	78.68	116.98	4475	139.60	1743	8.83	3-1/2
417	17		24.50	239.05	78.65	116.22	4610	140.60	1833	9.02	4
418	17		24.50	239.05	78.70	116.25	4610	139.60	1833	9.02	4

APPENDIX F

SUMMARY OF BIMETAL-TUBE DATA

BIMETALLIC TUBE DATA

Run No.	Tube Designation	Tube Characteristics	Steam Pressure (Corrected, psia)	Steam Temperature (°F)	Air-Inlet Temperature (Corrected °F)	Air-Outlet Temperature (Corrected °F)	Q (Btu/hr)	ΔT_{LM}	V_{max}	U_o	Orifice Size (in.)
494	3	A_o = 3.48	24.35	238.70	82.80	118.30	1885	139.00	811	3.89	2
495	3	A_{flow} = 0.0614	24.35	238.70	80.50	108.95	2220	143.00	1205	4.47	2-1/2
496	3		24.35	238.70	80.45	116.25	1880	140.00	825	3.86	2
497	3		24.35	238.70	80.25	107.70	2170	143.70	1210	4.35	2-1/2
498	3		24.35	238.70	80.70	104.35	2360	147.00	1529	4.61	3
499	3		24.35	238.70	81.05	101.95	2525	149.00	1860	4.86	4
500	4	A_o = 3.51 ft^2	24.05	237.92	84.40	116.08	4110	136.30	1860	8.59	4
501	4	A_{flow} = 0.0657 ft^2	24.05	237.92	82.86	116.27	4360	136.80	1861	9.09	4
502	4		24.05	237.92	83.33	120.74	3915	135.80	1495	8.22	3
503	4		24.05	237.92	84.07	126.94	3440	128.90	1148	7.61	2-1/2
504	4		24.05	237.92	84.95	137.57	2860	125.90	775	6.48	2
505	36	A_o = 3.665 ft^2	23.89	237.53	86.07	137.50	2755	123.90	763	6.06	2
506	36	A_{flow} = 0.0659 ft^2	23.89	237.53	85.55	127.25	3320	131.00	1137	6.90	2-1/2
507	36		23.89	237.53	86.65	122.10	3710	134.00	1450	7.55	3
508	36		23.89	237.53	85.80	118.10	4010	135.20	1770	8.09	4
510	54	A_o = 3.69 ft^2	24.15	238.20	81.45	117.33	3610	138.50	1480	7.27	3
511	54	A_{flow} = 0.064 ft^2	24.15	238.20	82.25	122.00	3180	135.80	1172	6.34	2-1/2
512	54		24.15	238.20	83.00	134.43	2750	126.90	786	5.88	2
513	54		24.15	238.20	81.00	114.10	4190	141.00	1800	8.05	4
514	54		24.10	238.05	83.75	116.60	4040	133.50	1800	8.20	4
515	54		24.10	238.05	84.15	120.65	3670	135.00	1475	7.36	3
517	38	A_o = 3.64 ft^2	24.00	237.80	84.27	125.40	2180	132.30	775	4.55	2
518	38	A_{flow} = 0.0642 ft^2	24.00	237.80	83.30	116.30	2565	137.50	1140	5.13	2-1/2
519	38		24.00	237.80	83.15	111.70	2860	140.50	1465	5.60	3
520	38		24.00	237.80	83.03	108.25	3065	144.30	1772	5.83	4

APPENDIX G

CALCULATION OF RUN NO. 481, USING SHORT-FORM, MODIFIED SHORT-FORM, LONG-FORM, AND MODIFIED LONG-FORM CALCULATION PROCEDURES

SHORT FORM

CONTROL UNIT DATA SHEET

Run No. 481

Date: 2/11/56

Tube Designation: All aluminum No. 16

Tube Characteristics:

Liner Material: None

A_o/A_i: 13.8 (assumed)

BWG : --

Fin O.D. : 2.021

Root O.D. : 1.143

Fins/inch : 9.017

Air Vel.		9400 ft / 4 min 21.8 sec											
Air Out		48.73°C = 119.73°F											
Air In		28.98°C = 84.20°F											
ΔT		19.75°C = 35.53°F											
Steam	10 + 14.11 = 24.11 psia, T = 238.1°F												

Avg. Slot Width: 2.021 Orifice Size: 4 in.

Calculations:

Anemometer Reading : 2158 ft/min

Correction : -81

Corr. Anemometer Rdg: 2077

Combined Steam, Metal and Fouling Resistance:

0.00085 (assumed)

Heat Load = $2077 \otimes 0.0872 \otimes \frac{530}{579.73} = 165.5 \otimes 1.06 \otimes 35.53 =$

$= 6230$ Btu/hr

LMTD: $238.1 - 84.20 = 153.90°F$

$238.1 - 119.73 = 118.37°F$

$r = \frac{153.90}{118.37} = 1.298$

Lnr = 0.2602

$U_{(\text{Liner O.D.})} = \frac{6230}{0.262 \otimes 136.2} = 174.5$

$\Delta T_{LM} = \frac{35.53}{0.2602} = 136.2°F$

$h_{(\text{Air-Liner O.D.})} = 205$ at 980 SFM

$\frac{1}{h_o} = \frac{1}{174.5} - 0.00085$

$= .00488$

MODIFIED SHORT FORM

CONTROL UNIT DATA SHEET

Date: 2/11/56 Run No. 481

Tube Designation: All aluminum No. 16

Tube Characteristics: Liner Material: None A_o/A_i: 13.8 (assumed)

BWG : --

Fin O.D. : 2.021

Root O.D. : 1.143

Fins/inch : 9.017

Air Vel.		9400 ft / 4 min 21.8 sec											
Air Out		48.73 - 0.04		=	48.69°C	=	119.65°F						
Air In		28.98 + 0.07 - 1.00		=	28.05°C	=	82.50°F						
ΔT					20.64°C	=	37.15°F						
Steam		10 + 14.11	=	24.11 psia	T =	238.10°F							

Avg. Slot Width: 2.021 Orifice Size: 4 in.

Calculations:

Anemometer Reading : 2158 ft/min

Correction : -81

Corr. Anemometer Rdg: 2077

Combined Steam, Metal and Fouling Resistance:

0.00085 (assume)

Heat Load = $\frac{2077}{1.52}$ ⊗ 0.0872 ⊗ $\frac{530}{579.65}$ = 109.0 ⊗ 1.06 ⊗ 37.15 =

= 4290 Btu/hr

LMTD: 238.1 - 82.50 = 155.60

238.1 - 119.65 = 118.45

$r = \frac{155.60}{118.45} = 1.315$

Ln 1.315 = 0.274

$U_{(\text{Liner O.D.})} = \frac{4290}{0.262 \otimes 135.5} = 120.5$

$\Delta T_{LM} = \frac{37.15}{0.274} = 135.5°F$

$h_{(\text{Air-Liner O.D.})}$ = 134 at 646 SFM

$\frac{1}{h_o} = \frac{1}{120.5} - 0.00085$

= 0.00745

LONG FORM

AIR TEST CALCULATION SHEET

Date of run: 2/11/56 Run No. 481

Tube Designation: All aluminum No. 16

Barometer: 732.2 mm Hg

Temperature: 20.2 °C

Test section: Tube Characteristics:

A_o: 3.58 ft² Orifice size 4 in. "dia

Anemometer reading 9,400 ft

A_{flow}: 0.0626 ft² Anemometer time 4 min 21.8 sec

Liner Material N

Rootwall Thickness 0.06 in.

Fin O.D. 2.021 in.

Root O.D. 1.143 in.

Fins/inch 9.017

T_{in} reading:	28.98	°C	T_{out} reading:	48.73	°C
Corr:	+0.07	°C	Corr:	-0.04	°C
T_{in}:	29.05	°C	T_{out}:	48.69	°C
T_{in}:	84.30	°F	T_{out}:	119.65	°F

P_{steam} = 10 psig + [(729.7) mm Hg x 0.01935] = 24.11 psia

T_{steam} = 238.1 °F (steam tables)

ΔT_1 = 238.1 - 84.30 = 153.80 °F $\quad \frac{\Delta T_1}{\Delta T_2}$ = 1.298

ΔT_2 = 238.1 - 119.65 = 118.45 °F $\quad \text{Ln} \frac{T_1}{T_2}$ = 0.2605

ΔT_{LM} = 135.4 °F $\quad \Delta t$ = 35.35 °F

$\frac{\rho}{\rho_o} = \left(\frac{729.7 \text{ mm Hg}}{579.65 \text{ °R}}\right) 0.6975 = 0.878$; $\sqrt{\frac{\rho}{\rho_o}}$ = 0.937

Anemometer reading: $\frac{9400 \text{ ft}}{(261.8) \text{ sec}} \times \frac{60 \text{ sec/min}}{} \sqrt{\frac{\rho}{\rho_o}} = 2020$ ft/min

Taylor correction: -69 ft/min

Std. ft of air flowing = $\frac{1951}{1.52}$ x = 1285

W = 1285 x 0.387 = 497 lbs/hr

Q = 498 x 35.35 x 0.24 = 4210 Btu/hr

$U_{o(\text{liner O.D.})} = \frac{(4210)}{0.262 \times (135.4)} = 118.5$

$U_{o(\text{outside area})} = 118.5 \times \frac{0.262}{(3.58)} =$ **8.68**

$V_{max} = 1285 \times \frac{0.0872}{(0.0626)} =$ **1790**

V_{face} = 672 ft/min and $h_{o(\text{liner O.D.})}$ = 131.5

$\frac{1}{U_o}$ = 0.00845 (on liner area)
.00085

$\frac{1}{h_o}$ = .00760

assuming all resistances except air film = 0.00085 (based on liner area).

MODIFIED LONG FORM

AIR TEST CALCULATION SHEET

Date of run: 2/11/56 Run No. 481

Tube Designation: All aluminum No. 16

Barometer: 732.2 mm Hg
Temperature: 20.2 °C
Liner Material N
Rootwall Thickness 0.06 in.
Fin O.D. 2.021 in.
Root O.D. 1.143 in.
Fins/inch 9.017

Test section: A_o: 3.58 ft^2 A_{flow}: 0.0626 ft^2

Tube Characteristics: Orifice size 4 in. "dia
Anemometer reading 9400 ft
Anemometer time 4 min 21.8 sec

T_{in} reading: 28.98 °C
Corr: -0.93 °C
T_{in}: 28.05 °C
T_{in}: 82.50 °F

T_{out} reading: 48.73 °C
Corr: -0.04 °C
T_{out}: 48.69 °C
T_{out}: 119.65 °F

P_{steam} = 10 psig + [(729.7) mm Hg x 0.01935] = 24.11 psia
T_{steam} = 238.1 °F (steam tables)

ΔT_1 = 238.1 - 82.50 = 155.6 °F

ΔT_2 = 238.1 - 119.65 = 118.45 °F

ΔT_{LM} = 135.5 °F Δt = 37.15 °F

$\frac{\Delta T_1}{\Delta T_2}$ = 1.315

$\text{Ln} \frac{T_1}{T_2}$ = 0.274

$\frac{\rho}{\rho_o} = \left(\frac{729.7 \text{ mm Hg}}{579.65 \ ^\circ R}\right) 0.6975 = 0.878$; $\sqrt{\frac{\rho}{\rho_o}}$ = 0.937

Anemometer reading: $\frac{9400 \text{ ft}}{(261.8) \text{ sec}}$ x 60 sec/min $\sqrt{\frac{\rho}{\rho_o}}$ = 2020 ft/min

Taylor correction: -69 ft/min

Std. ft of air flowing = $\frac{1951}{1.52}$ x = 1285

W = 1285 x 0.387 = 497 lbs/hr

Q = 497 x 37.15 x 0.24 = 4430 Btu/hr

$U_{o(\text{liner O.D.})} = \frac{(4430)}{0.262 \times (135.5)} = 124.8$

$U_{o(\text{outside area})} = 124.8 \times \frac{0.262}{(3.58)} = 9.13$

$V_{max} = \frac{1285}{} \times \frac{0.0872}{(0.0626)} = 1790$

$V_{face} = \frac{672}{}$ ft/min and $h_{o(\text{liner O.D.})}$ = 139.5

$\frac{1}{U_o}$ = 0.00802 (on liner area)
0.00085

$\frac{1}{h_o}$ = 0.00717

assuming all resistances except air film = 0.00085 (based on liner area).

APPENDIX H

CALCULATION OF BOND RESISTANCE VALUES FROM THE DATA FOR THE FIVE BIMETAL TUBES PRESENTED IN FIG. 13

Equation 43 can be arranged in the form

$$r_b = \frac{A_L}{A_o}\left[M'' - M_{\text{all al.}} - r_m\left(\frac{A_o}{A_m}\right)_{\text{bimetal}} + r_m\left(\frac{A_o}{A_m}\right)_{\text{aluminum}}\right] \quad (1\text{-H})$$

where

r_b = bond resistance of the tube,

A_L = heat transfer area of liner/ft length,

A_o = outside heat transfer area/ft length,

M'' = intercept value of line representing the bimetal (from Fig. 13),

$M_{\text{all al.}}$ = intercept value of all-aluminum tubes,

$r_m\left(\frac{A_o}{A_m}\right)_{\text{bimetal}}$ = metal resistance of bimetal tube, equals root wall plus liner resistance, and

$r_m\left(\frac{A_o}{A_m}\right)_{\text{aluminum}}$ = metal resistance of aluminum tube, equals root-wall resistance.

Assuming equivalent thickness in the average aluminum-tube root-wall thickness and the bimetal-tube root-wall thickness, Equation 1-H reduces to

$$r_b = \frac{A_L}{A_o}\left[M'' - M_{\text{all al.}} - \frac{X_L\, A_o}{K\, A_m}\right] . \quad (2\text{-H})$$

All of the five tubes have copper liners, therefore the liner resistance is computed for a 16 gage tube as

$$\frac{X_L A_o}{K A_m} = \frac{(0.065)(3.59)}{(220)(12)(0.25)}$$

$$= .000353.$$

The area ratio

$$\frac{A_L}{A_o} = \frac{0.262}{3.59} = \frac{1}{13.7} .$$

Substituting into Equation 2-H:

$$r_b = \frac{1}{13.7} [M'' - M_{\text{all al.}} - 0.000353] . \qquad (3\text{-H})$$

Tube No. 3:

The intercept value M" = 0.1045 (from Fig. 13).

The value of $M_{\text{all aluminum}} = 0.00481$.

Substituting the intercept values into Equation 3-H

$$r_b = \frac{1}{13.7} [0.1045 - 0.00481 - 0.000353]$$

$$= \frac{0.09934}{13.7} = 0.00725 .$$

Tube No. 38:

The intercept value M" = 0.0718 (from Fig. 13).

As before, $M_{\text{all al.}} = 0.00481$.

Substituting in Equation 3-H:

$$r_b = \frac{1}{13.7} [0.0718 - 0.00481 - 0.000353]$$

$$= \frac{.06664}{13.7} = 0.00485.$$

Tube No. 54:

The intercept value M" = 0.0220 (from Fig. 13).

$$M_{\text{all al.}} = 0.00481.$$

Substituting in Equation 3-H:

$$r_b = \frac{1}{13.7}[0.0220 - 0.00481 - 0.000353]$$

$$= \frac{.01684}{13.7} = 0.00123 .$$

Tube No. 36:

The intercept values

$$M'' = 0.0152$$

$$M_{\text{all al.}} = 0.00481.$$

Substituting in Equation 3-H:

$$r_b = \frac{1}{13.7}[0.0152 - 0.00481 - 0.000353]$$

$$= \frac{0.01004}{13.7} = 0.000733$$

Tube No. 4:

The intercept value for tube No. 4 is very close to that for the all-aluminum tubes and therefore the bond-resistance value is too small to be measured using the air-test apparatus.